

Non-Abelian Hybrid Fracton Orders

Nathanan Tantivasadakarn,^{1,*} Wenjie Ji,^{2,†} and Sagar Vijay^{2,‡}

¹*Department of Physics, Harvard University, Cambridge, MA 02138, USA*

²*Department of Physics, University of California, Santa Barbara, CA 93106, USA*

We introduce lattice gauge theories which describe three-dimensional, gapped quantum phases exhibiting the phenomenology of both conventional three-dimensional topological orders and fracton orders, starting from a finite group G , a choice of an Abelian normal subgroup N , and a choice of foliation structure. These hybrid fracton orders – examples of which were introduced in Ref. [1] – can also host immobile, point-like excitations that are non-Abelian, and therefore give rise to a protected degeneracy. We construct solvable lattice models for these orders which interpolate between a conventional, three-dimensional G gauge theory and a pure fracton order, by varying the choice of normal subgroup N . We demonstrate that certain universal data of the topological excitations and their mobilities are directly related to the choice of G and N , and also present complementary perspectives on these orders: certain orders may be obtained by gauging a global symmetry which enriches a particular fracton order, by either fractionalizing on or permuting the excitations with restricted mobility, while certain hybrid orders can be obtained by condensing excitations in a stack of initially decoupled, two-dimensional topological orders.

CONTENTS

I. Introduction	1
II. Example: 1-foliated (S_3, \mathbb{Z}_3) Gauge Theory	4
III. Conditions for mobility	6
IV. 1-foliated (G, N) gauge theory	8
V. 3-foliated (G, N) gauge theory	10
VI. Discussion	15
Acknowledgments	16
A. Review of Gauging and the Quantum Double model	16
B. Gauging G via minimal coupling	20
C. Examples of Symmetry Enrichment in Topological and Fracton Phases	21
D. Examples of 3-foliated hybrid models	24
References	26

I. INTRODUCTION

Non-Abelian anyons are exotic fractionalized excitations that arise in two-dimensional quantum systems with long-ranged entanglement, which provide promising avenues for performing fault-tolerant topological quantum computation[2]. A large class of non-Abelian anyons can

arise as the excitations of a gauge theory for a finite, non-Abelian gauge group G . Exactly solvable lattice models for these phases have provided insight into the universal properties of the gauge charges and fluxes in these states of matter [3, 4], which are in one-to-one correspondence with the irreducible representations (charges) and conjugacy classes (fluxes) of the group G . A generalization of these lattice models can be used to study the deconfined phases of G gauge theories in higher spatial dimensions [5–8].

More recently, novel states of matter where the gapped excitations have highly restricted mobility, called fracton orders, have been discovered in three spatial dimensions [9–13]. Fracton orders are similarly obtained by gauging a paramagnet with subsystem symmetry[13–19], defined as symmetry transformations along extensive sub-regions of the lattice. The X-cube model[13], for example, can be obtained from simultaneously gauging three intersecting planar symmetries.

A natural question to ask is whether one can similarly obtain novel phases which hosts non-abelian fracton excitations by “gauging” short-range-entangled systems with non-Abelian subsystem symmetry groups. In this general setting, it is generally not possible to gauge the full non-Abelian subsystem symmetry group; only an Abelian subgroup of the symmetry group can be gauged, thus giving rise to an Abelian fracton order¹. Other examples of non-Abelian fracton orders have been recently proposed, by strongly coupling non-abelian topological orders in 2D and 3D [20–25], by gauging the abelian subsystem symmetries in certain symmetry-protected topological phases [26, 27], or gauging a global symmetry which permutes fracton excitations in an abelian

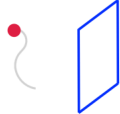
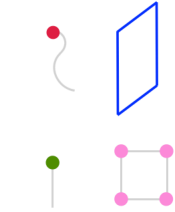
¹ Suppose the system of interest has three intersecting planar symmetries, each of which transforms a given plane under a non-abelian group G . The group commutator of two intersecting planar symmetries acts only on the intersection line. Therefore, the system has additional line symmetries given by the commutator subgroup $[G, G]$. Repeating the same argument with a third plane, we conclude that the system has a local symmetry $[G, G]$ at each site, and the only physical planar symmetry that can be gauged is the Abelian subgroup $G/[G, G]$.

* ntantivasadakarn@g.harvard.edu

† wenjieji@ucsb.edu

‡ sagar@physics.ucsb.edu

TABLE I. (G, N) **Gauge Theories:** For a given finite group G , the three-foliated (G, N) gauge theory constructed for different choices of normal subgroup N can realize hybrid fracton orders that interpolate between a three-dimensional G topological order and a pure fracton order. The gapped excitations in these orders above have mobilities which are indicated by the color-coding: a mobile gauge charge (red), a mobile flux loop (blue), fracton (pink) and lineon (green). For a one-foliated (G, N) gauge theory, the hybrid order contains planon excitations rather than lineons or fractons.

Group	G		
Normal subgroup	$N = \mathbb{Z}_1$	$\mathbb{Z}_1 \subset N \subset G$	$N = G$
Phase	G topological order	(G, N) hybrid order	Abelian G : G fracton order
Excitations			 Non-Abelian G : N/A

fracton order[28–32]. Nevertheless, a more general procedure for obtaining non-Abelian fracton orders given a non-Abelian symmetry group – in direct analogy with the two-dimensional quantum double – remains elusive.

In this work, we introduce a general construction to obtain topological quantum orders which host immobile, non-Abelian point-like excitations. These orders may be understood as the deconfined phase of an exotic gauge theory which is obtained by gauging a paramagnet with global symmetry group G along with subsystem symmetries of an abelian normal subgroup N arranged in a specified geometry. These two symmetries are not independent, since products of the subsystem symmetry transformation across distinct layers can generate a global symmetry transformation, which forms a normal subgroup of the global symmetry group G . We refer to the symmetry of such a paramagnet a *2-subsystem symmetry* denoted (G, N) and the long-range-entangled states that result from gauging such a symmetry (G, N) *gauge theories*. For a non-Abelian group G , there are choices of an Abelian normal subgroup N such that our construction yields a phase hosting non-Abelian fracton excitations.

We note that when the specified geometry of the subsystem symmetries in the short-range-entangled state consists of n sheaves of intersecting planes, we will refer to the (G, N) hybrid fracton order obtained by gauging these symmetries as *n-foliated*. We emphasize that this terminology only denotes the geometry of the symmetry group before the gauging procedure, and does not immediately imply that two dimensional topological orders can be “exfoliated” via a finite-depth quantum circuit from these (G, N) gauge theories. The latter definition of “foliated” fracton orders has been previously used in the literature[33–35].

The novelty of our construction is twofold. First, we demonstrate that (G, N) gauge theories simultaneously host both mobile point and loop excitations akin to the quantum double model, and point excitations with restricted mobility, as seen in fracton orders. This is illustrated in Table I. Because of the non-trivial fusion and braiding of these two types of ex-

citations, the (G, N) gauge theories obtained cannot be in the same phase as the tensor product of a pure 3+1d topological order and a pure fracton order. We note that particular examples of (G, N) gauge theories for Abelian G were explored in Ref. [1], where it was shown that the resulting orders exhibit a “hybrid” phenomenology, and host both excitations resembling those of a G/N gauge theory and those of an Abelian fracton order based on subsystem symmetry group N .

In addition, we argue a general relation between the properties of the groups G and N to the features of the fractionalized excitations in the (G, N) gauge theory. A certain set of point-like excitations (“charges”) transform as irreducible representations (irreps) of G , while another set of excitations (“fluxes”) are labeled by conjugacy classes of G , reminiscent of the labeling of excitations in the two-dimensional quantum double. Importantly, a key property we argue is that the irreps that correspond to non-trivial irreps of $Q \cong G/N$ are fully mobile excitations, and otherwise are fully immobile. Similarly, conjugacy classes that correspond to non-trivial conjugacy classes of Q are loop excitations, and otherwise are point excitations with restricted mobility.

To concretely study these properties, we construct an exactly solvable commuting projector model for any choice of input groups (G, N) and for which the planar subsystem symmetries intersect in a specified geometry. For the case of three intersecting planar symmetries (as in the construction of the X-cube model), our Hamiltonian takes the general form

$$H_{(G,N)} = - \sum_v \mathbf{A}_v^G - \sum_{r=x,y,z} \sum_{c,r} \mathbf{B}_c^N - \sum_p \mathbf{B}_p^Q. \quad (1)$$

Here, violations of \mathbf{A}_v^G for each vertex and point charges, where, depending on the type, can be either fractons or fully mobile. Furthermore, violations of \mathbf{B}_p^Q are loop excitations, and those of $\mathbf{B}_{c,r}^N$ are lineons, which are mobile in the direction \hat{r} . When the subsystem symmetries of the paramagnet lie along parallel planes (1-foliated), we are also able to derive the operators which create specific excitations in the corresponding (G, N) gauge theory.

TABLE II. **Three-foliated, hybrid fracton orders corresponding to groups $G = \mathbb{Z}_4, S_3, D_4,$ and $Q_8,$ and an indicated choice of normal subgroup.** The fracton excitations in (G, N) gauge theories are labeled by irreducible representation (irreps) of G . Here, $s,$ and r are different sign representations, while $\mathbf{2}$ is a two-dimensional irreducible representation of G . Finally, e is the generating irrep of \mathbb{Z}_4 . References are included for models that have appeared in previous works.

G	N	Fractons		Refs.
		Non-Abelian	Abelian	
\mathbb{Z}_4	\mathbb{Z}_2	-	e	[1]
S_3	\mathbb{Z}_3	$\mathbf{2}$	-	[36]
D_4	\mathbb{Z}_2	$\mathbf{2}$	-	[22]
	\mathbb{Z}_2^2	$\mathbf{2}$	s, rs	[27–29, 36]
	\mathbb{Z}_4	$\mathbf{2}$	r, rs	-
Q_8	\mathbb{Z}_2	$\mathbf{2}$	-	-
	\mathbb{Z}_4	$\mathbf{2}$	r, rs	-

The solvable Hamiltonian includes, as limiting cases, both conventional fracton orders and the three-dimensional quantum double. Specifically, when the group $N = \mathbb{Z}_1$, the model reduces to the $3 + 1d$ quantum double model of G on a cubic lattice. When the global symmetry group G is Abelian, and $N = G$, the model is equivalent to a fracton order with subsystem symmetry gauge group N . It is when Q and N are both non-trivial groups and when G is a non-trivial extension of Q by N that we find the presence of hybrid orders, which provide an interplay between topological order and fracton orders.² Such a hybrid model always hosts non-Abelian fractons when G is non-Abelian. That is, there exists irreducible representations of G with dimension greater than one that displays restricted mobility.

By systematically studying (G, N) gauge theories, our work provides a unified way of obtaining non-Abelian fracton orders studied in the literature, while also yielding new fracton orders. Many previous non-Abelian fracton orders that have been considered correspond to (G, N) gauge theories, where the non-Abelian group G takes the particular form $G \cong N \rtimes Q$ where N is an Abelian group. Physically, these orders are obtained by starting with an Abelian fracton order (with gauge group N) whose excitations are permuted under the action of a global symmetry group Q , and then gauging this permutation symmetry. The difficulty in these previous examples is that for each (G, N) symmetry pair, one needs to design Abelian fracton models with the desired enriching symmetry. The difficulty is resolved using our construction.

The (D_4, \mathbb{Z}_2^2) gauge theory reproduces the model in Refs. 27–29, where the symmetry that exchanges a pair of \mathbb{Z}_2 X-cube models is gauged, or by gauging an SPT with protected by both a \mathbb{Z}_2 global symmetry and a \mathbb{Z}_2^2 subsystem symmetry. The (D_4, \mathbb{Z}_2) gauge theory produces the same excitations found in the D_4 defect network model constructed in Ref.

22. We show that the (D_4, \mathbb{Z}_4) gauge theory is a third model which hosts D_4 non-Abelian fractons, previously conjectured in Ref. 28. We explicitly construct this model and confirm that it can be obtained from gauging the charge conjugation symmetry of the \mathbb{Z}_4 X-cube model.

Non-Abelian groups G that arise from a general group extension can also be chosen, yielding a rich array of non-Abelian fracton orders that have not been previously studied. An example we explicitly construct is a model with Q_8 (quaternion) non-abelian fractons, which cannot be obtained by gauging a symmetry that only permutes or fractionalizes the fracton excitations³. In Table II, we list the non-abelian and abelian fractons that appear in the hybrid fracton order for various choices of G and N .

A number of open questions remain about the nature of hybrid fracton orders and (G, N) gauge theories. First, the behavior of the hybrid orders presented here under entanglement renormalization[37, 38] is not known. In particular, it is not apparent if the foliation structure of the N subsystem symmetries in a short-range-entangled state implies that two-dimensional topological orders can be exfoliated from the corresponding (G, N) gauge theory using a finite-depth quantum circuit [33–35]. Second, within our construction it is not possible to obtain an order with non-Abelian fractons but without mobile or loop-like excitations. Whether this exists as a possibility outside of the gauge theoretic framework remains an open question. Furthermore, one possibility not considered in this work is that the short-range-entangled states can be put into a symmetry-protected topological order with respect to the (G, N) symmetry before gauging. The properties of such twisted hybrid fracton orders are outside the scope of this work. Third, (G, N) gauge theories based on continuous groups remain to be systematically studied. Fourth, for 1-foliated (G, N) gauge theories with non-Abelian loop excitations, the loops generally exhibit a quantum dimension which grows exponentially in the loop length. The universal properties of this excitation (e.g. three-loop braiding) remain to be explored, as well as possible uses of these excitations for robust quantum information storage and computation. Finally, it would be interesting to see a general field theory construction for (G, N) gauge theories. For the case of a central extension, we believe such theories have been realized recently in Ref. 39.

A. Summary

We now provide an outline of our paper. The first part of this work studies (G, N) gauge theories which give rise to 1-foliated fracton orders. In this case, the short-range-entangled state exhibits subsystem symmetries along non-intersecting planes. The foliation structure of the resulting gauge theory is

² When G is a trivial extension of Q by N , the model is a tensor product of a Q quantum double model and a fracton order with subsystem symmetry gauge group N .

³ Mathematically, this follows from the fact that the group extension

$$1 \rightarrow \mathbb{Z}_4 \rightarrow Q_8 \rightarrow \mathbb{Z}_2 \rightarrow 1$$

is neither central nor split.

also apparent from a complementary constructions, by starting with a decoupled stack of two-dimensional G gauge theories, and proliferating an appropriate set of gapped excitations that couple the layers together.

In Sec. II, we present the detailed properties of a non-Abelian one-foliated (G, N) gauge theory with $(G, N) = (S_3, \mathbb{Z}_3)$ in detail⁴. In addition to non-abelian point-like excitations which are restricted to move within planes (planons), the resulting order contains a loop-like excitation with a quantum dimension that grows exponentially in its length.

The intricate connection between the choice of groups G and N and the properties of the excitations in the one-foliated gauge theory are clarified by studying the properties of the (D_4, N) gauge theories, where D_4 (the dihedral group of eight elements) admits three distinct normal subgroups N . Each choice leads to different mobility constraints of the excitations. More generally, for the one-foliated (G, N) gauge theories, we demonstrate a general connection between G, N and the properties of the deconfined excitations in Sec. III. We show that, like the quantum double model, these gauge theories admit excitations which are labeled by irreducible representations (irreps) of G (charges) and conjugate excitations (fluxes) which are labeled by conjugacy classes of G , in analogy with the three-dimensional gauge theories with finite group G . In addition, however, we show that given the projection map from G to the quotient group Q ,

1. A charge excitation is mobile iff the corresponding irrep of G can be pulled back from a non-trivial irrep in $Q \cong G/N$. Otherwise the charge has restricted mobility.
2. A flux corresponding to a conjugacy class of G is a loop-like excitation iff the conjugacy class is non-trivial when pushed forward to Q . Otherwise, the flux is point-like, with restricted mobility.

A detailed description of these conditions, as well as the conditions for mobile charge and flux loop excitations is provided in Sec. III.

In Sec. IV, we present an exactly solvable model for a 1-foliated (G, N) gauge theory, for an arbitrary choice of G and N . We also verify the properties of the charges and fluxes explicitly by constructing the operators which create these excitations.

In Sec. V, we present a commuting projector model whose ground state realizes any 3-foliated (G, N) gauge theory. We argue that the same relationship between G, N , and the mobility of the emergent excitations in the 1-foliated (G, N) gauge theory, holds for the 3-foliated case. The 3-foliated gauge theory has no obvious condensation picture, especially because there is no known fracton model with non-abelian gauge group. We demonstrate that the charge excitations are in correspondence with irreps of G , and we observe the mobility constraints of these excitations explicitly by studying the lattice Hamiltonian.

II. EXAMPLE: 1-FOLIATED (S_3, \mathbb{Z}_3) GAUGE THEORY

In this section, we discuss the simplest non-abelian group $G = S_3$, for which the only proper and non-trivial normal subgroup is $N = \mathbb{Z}_3$. Our discussion here will follow very closely to that of the 1-foliated $(\mathbb{Z}_4, \mathbb{Z}_2)$ gauge theory (i.e. the hybrid toric code layers of Ref. 1).

A. (S_3, \mathbb{Z}_3) paramagnet

We start with a short range entangled (SRE) phase, consisting of L independent copies of a two-dimensional paramagnet with $S_3 = \langle r, s | r^3 = s^2 = (sr)^2 = 1 \rangle$ symmetry (for example, the paramagnet of the 3-states Potts model). The full symmetry group of the stacked layers is S_3^L . The elementary charged excitations in each layer transform under irreducible representations (irreps) of S_3 . The irreps are

1. **1**: the trivial irrep of dimension 1
2. **s** : the sign irrep of dimension 1
3. **2**: the faithful irrep of dimension 2

The non-trivial fusion rules of the charges are given by

$$\mathbf{s} \otimes \mathbf{s} = \mathbf{1}, \quad (2)$$

$$\mathbf{2} \otimes \mathbf{2} = \mathbf{1} \oplus \mathbf{s} \quad (3)$$

Next, we will explicitly break the symmetry from S_3^L down so that each layer only has a \mathbb{Z}_3 symmetry, while retaining a global S_3 symmetry. This can be done by adding couplings between adjacent layers that allow only the charges s to tunnel between layers. The global symmetry – defined as the product of S_3 symmetries in all layers – is still preserved, and so we can still label the charged excitations as irreps of S_3 . However, because we no longer have conservation of s in each layer, the subsystem symmetry is broken down to $N = \mathbb{Z}_3$ in each plane. Under this subgroup, we note that s transforms trivially, which is consistent with the fact that it is allowed to hop between layers. Furthermore, the 2D irrep **2** reduces down to a direct sum of the two non-trivial irreps of \mathbb{Z}_3 (which we will call ω and $\bar{\omega}$). Importantly, since it is still a non-trivial representation under N , the **2** excitation is a planar excitation. However, Eq. (3) implies that the outcome of fusing two **2** excitations is always mobile.

Let us now gauge the remaining symmetry of the paramagnet. The properties of the charge excitations of the SRE state carry over to the gauge charges of the resulting hybrid order. Qualitatively, we first gauge the \mathbb{Z}_3 planar symmetries to obtain a stack of \mathbb{Z}_3 toric codes, where the irreps ω and $\bar{\omega}$ of the \mathbb{Z}_3 symmetry are promoted to the anyons e and \bar{e} , respectively in each layer. The global symmetry is now reduced to the quotient group $Q = G/N = \mathbb{Z}_2$, which acts as charge conjugation on the toric code anyons as $e \leftrightarrow \bar{e}$ and $m \leftrightarrow \bar{m}$, where the bar denotes the antiparticle. Because of this, the global symmetry enriches the stack of \mathbb{Z}_3 toric codes. Finally, we can gauge the Q global symmetry. The charges s of Q

⁴ The simplest non-trivial abelian model is $(\mathbb{Z}_4, \mathbb{Z}_2)$ and has been presented in Ref. 1.

TABLE III. **Summary of excitations in stacks of $\mathcal{D}(S_3)$ and the 1-foliated (S_3, \mathbb{Z}_3) gauge theory.** The same labels can be used for the excitations in both models. The quantum dimension d for each type of excitation is listed.

Excitation label	$\mathcal{D}(S_3)$ stacks		(S_3, \mathbb{Z}_3)	
	Type	d	Type	d
$(1_1, \mathbf{1}) \equiv \mathbf{1}$	mobile	1	mobile	1
$(1_1, \mathbf{s}) \equiv \mathbf{s}$	planon	1	mobile	1
$(1_1, \mathbf{2}) \equiv \mathbf{2}$	planon	2	planon	2
$(1_r, \mathbf{1}) \equiv 1_r$	planon	2	planon	2
$(1_r, \boldsymbol{\omega})$	planon	2	planon	2
$(1_r, \bar{\boldsymbol{\omega}})$	planon	2	planon	2
$(1_s, \mathbf{1}) \equiv 1_s$	planon	3	loop	3^{2l}
$(1_s, \mathbf{s})$	planon	3	loop	3^{2l}

are promoted to gauge charges of the hybrid model, while the superposition of e and \bar{e} in each layer is promoted to the non-abelian particle $\mathbf{2}$ of the hybrid model.

Nevertheless, to study the flux excitations, we find it more enlightening to consider an alternative construction of this hybrid model via a condensation transition. First, we temporarily neglect the interlayer couplings and gauge the full S_3^L symmetry of the stacked 2D paramagnets. The result is a stack of L quantum double models $\mathcal{D}(S_3)$. There are eight types of anyons in each layer, which can be labeled by a conjugacy class and an irrep of the corresponding centralizer, as summarized in Table III. Note that when either the conjugacy class or irrep is trivial, we will often refer to the excitation using its other non-trivial label. Such excitations, are the pure charges and pure fluxes of the model, respectively.

To recover the hybrid model, we can recover the interlayer hoppings by inducing a condensation transition between a pair of s anyons in every adjacent layer. As a consequence, the s in each layer are now in the same superselection sector in the condensate phase, making the s particle mobile. Now, the pure flux 1_s braids non-trivially with s , and is therefore confined. However, a composite loop excitation, composed of a pair of 1_s excitations in each layers braids trivially with the condensate, and therefore remains deconfined. We will use the same label of the original anyon to label this loop excitation in the hybrid model. That is, we will call this the “ 1_s loop”.

Before investigating the properties of the loop let us first argue that this loop excitation does not fuse into anything that forms the condensate, and therefore does not split. First, consider the following fusion rule for two 1_s anyons

$$1_s \otimes 1_s = \mathbf{1} \oplus \mathbf{2} \oplus 1_r \oplus (1_r, \boldsymbol{\omega}) \oplus (1_r, \bar{\boldsymbol{\omega}}). \quad (4)$$

We see that the fusion outcomes do not involve the charge s . Similarly, the fusion of 1_s with all the other anyons except s and $(1_s, s)$ (the bound state of the two) does not involve s . This guarantees that the fusion 1_s loop with some other excitation not involving s will have at most one trivial superselection sector as a fusion outcome. Thus, after condensing pairs of s in adjacent layers, the fusion of the 1_s loop with the remaining deconfined particles will have a unique trivial superselection sector. This guarantees that the 1_s loop does not

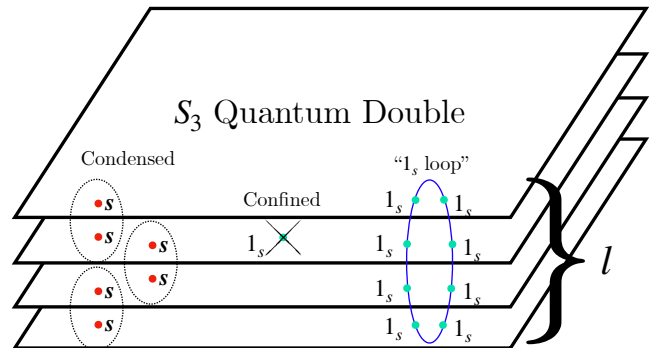


FIG. 1. Alternative construction of the 1-foliated (S_3, \mathbb{Z}_3) hybrid model via a condensation of s pairs in adjacent $\mathcal{D}(S_3)$ layers. As a result, the flux 1_s is confined, but a flux loop composed of 1_s pairs in l layers survives the transition. The quantum dimension of this loop excitation is 3^{2l} .

split.

We can now discuss the peculiar properties of the 1_s flux loop. First, since the 1_s anyon before the condensation has quantum dimension 3, the resulting flux loop has quantum dimension 3^{2l} , where l is the number of layers in which the flux loop pierces⁵. This extensive quantum dimension can be seen explicitly by fusing two identical flux loops. Following Eq. (4), the fusion of two identical 1_s loops in the hybrid order will result a product of the given fusion outcomes at the $2l$ points where the loop pierces a 2d layer.

Let us remark that “shape dependence” of the quantum dimension of such flux loops was pointed out in Refs. 28 and 29 in a model with three foliations. For 1-foliated hybrid models, this curious property is demystified from the condensation construction. In fact, one can see what happens to the quantum dimension when we shrink the loop excitation so that the number of layers pierced decreases by one. In the layer where the loop no longer pierces, shrinking the loop away is just equivalent to fusing two 1_s anyons away before the condensation, and therefore in that layer, we will be left with the planons $\mathbf{1} \oplus \mathbf{2} \oplus 1_r \oplus (1_r, \boldsymbol{\omega}) \oplus (1_r, \bar{\boldsymbol{\omega}})$. This decreases the quantum dimension of the loop by 3^2 .

Lastly, it is perhaps worth pointing out the nature of the loop excitation $(1_s, s)$ in the hybrid model. This is simply the bound state of the mobile particle s and the loop 1_s . Indeed, the fusion rules are identical to the anyons of $\mathcal{D}(S_3)$:

$$1_s \otimes s = (1_s, s). \quad (5)$$

This bound state is well-defined because both excitations are fully mobile.

⁵ In general, the flux loop can pierce a layer multiple times, in which case we must count all the number of pierces.

III. CONDITIONS FOR MOBILITY

In this section, we will state the conditions for which a charge of the hybrid fracton model will have restricted mobility in terms of the input data G and N . First, we give examples of a 1-foliated (D_4, N) Gauge Theory in Sec. III A. In contrast to the $(\mathbb{Z}_4, \mathbb{Z}_2)$ model in Ref. 1 and (S_3, \mathbb{Z}_3) in the previous section, there are multiple non-trivial normal subgroups for D_4 . We will point out how this choice is reflected in the mobility of the particles, which in turns uniquely determines the type of anyons we have to condense in the layer construction. Then, in Sec. III B we give a precise statement of the mobility constraints for a general choice of G and N .

A. 1-foliated (D_4, N) Gauge Theory

We consider the dihedral group $G = D_4 \equiv \langle r, s | r^4 = s^2 = (sr)^2 = 1 \rangle$. The quantum double model $\mathcal{D}(D_4)$ consists of 22 anyons. For simplicity, we will only discuss the pure charge and flux excitations. There are five pure charges given by the different irreps of D_4 : the trivial irrep $\mathbf{1}$, the 2D faithful irrep $\mathbf{2}$, and three sign reps

1. s with kernel $\mathbb{Z}_4 = \langle r \rangle$
2. r with kernel $\mathbb{Z}_2^2 = \langle r^2, rs \rangle$
3. rs with kernel $\mathbb{Z}_2^2 = \langle r^2, s \rangle$

The sign reps have an abelian $\mathbb{Z}_2^2 = D_4/\mathbb{Z}_2$ fusion rules and are labeled by a representative element under the quotient group. They can be absorbed into $\mathbf{2}$ by fusion. Lastly, the fusion of two $\mathbf{2}$ irreps is given by

$$\mathbf{2} \otimes \mathbf{2} = \mathbf{1} \oplus \mathbf{s} \oplus \mathbf{r} \oplus \mathbf{rs} \quad (6)$$

The fluxes are labeled by conjugacy classes of D_4 , which we label by representative elements as $1_1, 1_{r^2}, 1_r, 1_s, 1_{rs}$. They satisfy more involved fusion rules, so we will just note that $1_r, 1_s$, and 1_{rs} are non-abelian fluxes of quantum dimension two, and 1_{r^2} is an abelian flux of order two.

We will now demonstrate for the case of (D_4, N) that the resulting hybrid model depends on the choice of N . Note that in contrast, for a 2D model (i.e. the single layer limit), the resulting topological order $\mathcal{D}(D_4)$ – obtained by first gauging N followed by gauging the quotient group $Q = G/N$ – does not depend on the choice of N .

We start with L layers of a paramagnet each invariant under D_4 . Again, there are two ways to construct the hybrid model. The first is to add charge-hopping terms to reduce the symmetry from D_4^L down to (D_4, N) . One can then gauge the remaining symmetry. Alternatively, one can first gauge the D_4 symmetry in each layer to obtain a stack of D_4 quantum double models. Then, condense pairs of appropriate gauge charges that we want to make mobile. Let us see what the resulting type of excitations we get for each choice of N .

1. $N = \mathbb{Z}_1, Q = D_4$. The resulting model in this case is the usual D_4 gauge theory in 3D, since the subsystem

symmetry N is trivial. All charges are mobile. Therefore, in the layer construction, we can achieve this by condensing pairs of all gauge charges in adjacent layers.

2. $N = \mathbb{Z}_2, Q = \mathbb{Z}_2^2$. We begin with the (D_4, N) paramagnet and first gauge the N planar symmetries. This results in layers of \mathbb{Z}_2 toric codes enriched by a global Q symmetry. In particular, Q acts projectively on the charge e , but acts trivially on m .

We next gauge Q to obtain the (D_4, \mathbb{Z}_2) gauge theory. Since e transforms projectively, it is promoted to a particle of quantum dimension 2, in each layer, which we can identify as $\mathbf{2}$. Moreover, the mobile charges under Q are promoted to mobile gauge charges, which are the irreps r, s, rs . Therefore, we see that this hybrid model can be obtained in the layered construction by condensing pairs of all sign reps in adjacent layers of $\mathcal{D}(D_4)$.

To complete the discussion, we discuss the nature of the fluxes. Since Q does not act projectively on m , it is not affected by the gauging, and remains an abelian planon of order two. Thus, we can identify it with 1_{r^2} . The remaining flux loops, which are promoted symmetry defects of Q must therefore be labeled by $1_r, 1_s, 1_{rs}$ and are non-abelian. In the layered construction, the loop excitations are respectively constructed by a product of the anyons $1_r, 1_s$, and 1_{rs} of the original $\mathcal{D}(D_4)$ in each layer, which remains deconfined after the condensation of the three sign rep pairs. All flux loops have quantum dimension 2^{2l} .

3. $N = \mathbb{Z}_4, Q = \mathbb{Z}_2$. Gauging the N planar symmetry in the paramagnet results in a stack of \mathbb{Z}_4 toric codes. The remaining global symmetry is $Q = \mathbb{Z}_2$, which acts as “charge conjugation” by permuting the anyons $e \leftrightarrow \bar{e}$ and $m \leftrightarrow \bar{m}$ in each layer. Gauging Q promotes of e and \bar{e} into a single non-abelian planon $\mathbf{2}$, while e^2 is promoted to planon r . The mobile charge of Q corresponds to a mobile charge s , while rs is a bound state of r and s , and is therefore a planon. Therefore, this model can be obtained in the layered construction by condensing pairs of s in adjacent layers.

To see the mobility of the fluxes, we note that the \mathbb{Z}_2 symmetry does not permute m^2 , so it remains an abelian planon, which we must identify with the flux 1_{r^2} . On the other hand, since Q exchanges m and \bar{m} , their superposition gets promoted to a non-abelian planon, labeled by 1_r . The 1_s and 1_{rs} anyons in the original $\mathcal{D}(D_4)$ model are confined, and only a string of them are deconfined, which forms loop excitation of the same label.

4. $N = \mathbb{Z}_2^2$. Without loss of generality, we choose $N = \langle r^2, rs \rangle$.⁶ Gauging the \mathbb{Z}_2^2 planar symmetry in the para-

⁶ The case $N = \langle r^2, s \rangle$ gives an identical model because of the automorphism $s \rightarrow rs$, which swaps irreps $r \leftrightarrow rs$ and conjugacy classes $1_s \leftrightarrow 1_{rs}$.

TABLE IV. Summary of pure charges and fluxes for the 1-foliated model $G = D_4$ with different choices of N . Here \cdot = mobile point, p = planon, and \circ = mobile loop. Note that $\mathbf{2}$, 1_s , 1_r , 1_{rs} are non-abelian excitations, with possibly restricted mobility, depending on N . The two $N = \mathbb{Z}_2^2$ differ by a choice of the embedding $\iota: N \rightarrow G$ in the group extension (7), but the resulting models are equivalent up to relabeling the excitations. In the 3-foliated model, the charges and fluxes with restricted mobility are instead fractons and lineons, respectively.

excitation	N				
	\mathbb{Z}_1	\mathbb{Z}_2	\mathbb{Z}_4	\mathbb{Z}_2^2	\mathbb{Z}_2^2
\mathbf{s}	\cdot	\cdot	\cdot	p	p
\mathbf{r}	\cdot	\cdot	p	\cdot	p
\mathbf{rs}	\cdot	\cdot	p	p	\cdot
$\mathbf{2}$	\cdot	p	p	p	p
1_s	\circ	\circ	\circ	\circ	p
1_r	\circ	\circ	p	\circ	\circ
1_{rs}	\circ	\circ	\circ	p	\circ
$1_{r,2}$	\circ	p	p	p	p

magnet results in bilayers of \mathbb{Z}_2 toric codes where the twist defects 1_{rs} and $1_{r,2}$ become the anyons m_1 and m_2 . The remaining global symmetry is $Q = \mathbb{Z}_2$, which permutes the anyons $e_1 \leftrightarrow e_2$ and $m_1 \leftrightarrow m_2$. Gauging Q promotes the “superposition” of e_1 and e_2 into the planon $\mathbf{2}$, while $e_1 e_2$ is promoted to the planon \mathbf{rs} . The mobile charge of Q gauges to \mathbf{r} , and its bound state with \mathbf{rs} is another planon \mathbf{s} . Therefore, we see that model can be obtained in the layered construction by condensing pairs of \mathbf{r} in adjacent layers.

The global Q symmetry acts trivially on $m_1 m_2$, so it remains a planon $1_{r,2}$. The superposition of m_1 and m_2 becomes a non-abelian planon 1_{rs} . Finally, 1_s and 1_r are loop excitations, which can be seen as a product of 1_s and 1_r anyons in each layer, which braids trivially with pairs of \mathbf{r} in the layer construction.

A summary of the mobility of the pure charges and fluxes for different choices of N is given in Table IV.

B. Mobilities of excitations

We now consider a hybrid fracton model corresponding to choice (G, N) and an arbitrary geometry of the subsystem symmetries. We will make the assumption that pure charges of this model can be labeled by irreps of G , and that the pure fluxes can be labeled by conjugacy classes of G . (We show in Sec. IV that this holds for the 1-foliated case by explicitly constructing the excitations in an exactly solvable model. For the 3-foliated case, we can only rigorously show the former, and for now we conjecture the latter to be true)

Accepting such assumption, we are able to show the following. Given the group extension

$$1 \rightarrow N \xrightarrow{\iota} G \xrightarrow{\pi} Q \rightarrow 1 \quad (7)$$

1. Irreps of G that can be pulled back⁷ from Q correspond to mobile charges
2. Irreps of G that are non-trivial⁸ when pulled back to N correspond to charges with restricted mobility.
3. The conjugacy classes of G whose union forms $\iota(N)$ correspond to fluxes with restricted mobility.
4. The preimage of conjugacy classes of Q under π correspond to flux loops.

First, to argue Claim 2, recall that the nature of the restricted mobility of fractons is due to a conservation law in the fracton model. This conservation law arises from gauging subsystem symmetries, which disallows a single charge to move outside the support on which the subsystem symmetry acts[18]. Similarly, we see that any irrep of G that transforms non-trivially under (pulling back to) N will be charged under the N subsystem symmetries of the model, and after the duality, must result in a charge excitation with restricted mobility.

Claim 1 is cleanest to see after gauging the N planar symmetries, where only Q remains as the global symmetry. It follows that any charge under Q must be mobile since there is no extra conservation law preventing Q charges to move between planes.

For completeness, we must show that the two conditions above do not overlap. That is, for each irrep of G , exclusively only either claim 1 or claim 2 applies. To show this, we use the fact that the exact sequence (7) induces a dual short exact sequence

$$0 \leftarrow \hat{N} \xleftarrow{\hat{\iota}} \hat{G} \xleftarrow{\hat{\pi}} \hat{Q} \leftarrow 0 \quad (8)$$

where $\hat{G} \equiv \text{Hom}(G, \mathbb{C})$ is the Pontryagin dual consisting of characters of G . Since $\ker \hat{\iota} = \text{im } \hat{\pi}$, any irreducible character of G is trivial when pushed via $\hat{\iota}$ to a character of N iff it can be pushed from a character of Q via $\hat{\pi}$.

Moving on to the fluxes, in Claim 3, the conjugacy classes whose union forms N correspond to the subsystem symmetry defects of N . Upon gauging N , they become fluxes with restricted mobility. We can also see which of these fluxes are non-abelian. Conjugacy classes that contain elements from multiple conjugacy classes of N are those that become non-abelian after gauging Q . We remark that if the extension is central, then all such fluxes will be abelian.

Finally, for Claim 4, we see that the preimage of conjugacy classes of Q correspond to symmetry defects that are not promoted to flux excitations after gauging N . Therefore, they are defects of a global symmetry Q and are therefore loop-like.

Similarly to the charges, for each conjugacy class only one of Claim 3 or Claim 4 will apply because of the exactness of the group extension (7). That is, any flux excitation can

⁷ Given a group homomorphism $G \xrightarrow{\pi} Q$, the pullback of a representation U^q is given by $U^{\pi(g)}$. Furthermore, since π is surjective, an irrep of Q pulls back to a unique irrep of G .

⁸ but not necessarily irreducible

be uniquely labeled as either be a loop excitation or a point excitation with restricted mobility.

To give concrete examples, we demonstrate that the (D_4, N) models we considered Sec. III A are consistent with our claims. For brevity, we use the adjective “restricted” to refer to an excitation with restricted mobility.

1. $N = \mathbb{Z}_1$. Since N is trivial, $G = Q$ and therefore irreps of G can be pulled back from Q , and are therefore all mobile. Similarly, all conjugacy classes of G can be pushed forward to Q , and are hence loop excitations.
2. $N = \mathbb{Z}_2$. The three sign reps correspond to charges of Q , and are therefore all mobile, while $\mathbf{2}$ pulls back to the sign rep of N , and is therefore restricted. For fluxes, the non-trivial conjugacy class of N pushes forward to the conjugacy class $1_{r,2}$ of D_4 , so only this flux has restricted mobility (and is abelian). The remaining non-trivial conjugacy classes are preimages of conjugacy classes in Q and so are loop excitations. We find that the mobility conditions of this gauge group for the 3-foliated case is consistent with the model with D_4 non-abelian fractons presented in Ref. 22 using the defect network construction.
3. $N = \mathbb{Z}_4$. The irrep $\mathbf{2}$ pulls back to a 2D reducible representation $\omega \oplus \bar{\omega}$ of N , while r , and rs pull back to the irrep ω^2 . Therefore, the irreps $\mathbf{2}$, r , and rs all have restricted mobility. On the other hand, s can be pulled back from the sign rep of Q and is therefore mobile. For fluxes, the conjugacy class $1_{r,2}$ in N maps to $1_{r,2}$ in G , while 1_r and $1_{r,3}$ in N maps to a single conjugacy class 1_r in G . Therefore, $1_{r,2}$ and 1_r are restricted, the latter being non-abelian. The conjugacy classes 1_s and 1_{rs} map to the non-trivial conjugacy class in Q , so such fluxes are mobile loops.
4. $N = \mathbb{Z}_2^2$. The irreps $\mathbf{2}$, s , and rs are restricted, since they pull back to charges $(-1, -1)$, $(1, -1)$, and $(1, -1)$ of $N = \mathbb{Z}_2^2$ while r can be pulled back from the sign rep of Q , so it is mobile. For fluxes, there are three non-trivial conjugacy classes of N , one of which maps to $1_{r,2}$ and two of which maps to 1_{rs} . Therefore, these conjugacy classes are fluxes with restricted mobility, the latter being non-abelian. The conjugacy classes 1_s and 1_r map to the non-trivial conjugacy class in Q , so such fluxes are mobile loops. The mobility conditions of this gauge group for the 3-foliated case is consistent with the D_4 model obtained by gauging the SWAP symmetry of two X-cube models[28, 29].

IV. 1-FOLIATED (G, N) GAUGE THEORY

In this section, we present an exactly solvable model for the 1-foliated (G, N) gauge theory, which can be thought of as a hybrid between a 3D quantum double model and a stack of 2D quantum double models[3, 6]. The case where $(G, N) = (\mathbb{Z}_4, \mathbb{Z}_2)$ is the hybrid toric code layers presented in Ref. 1.

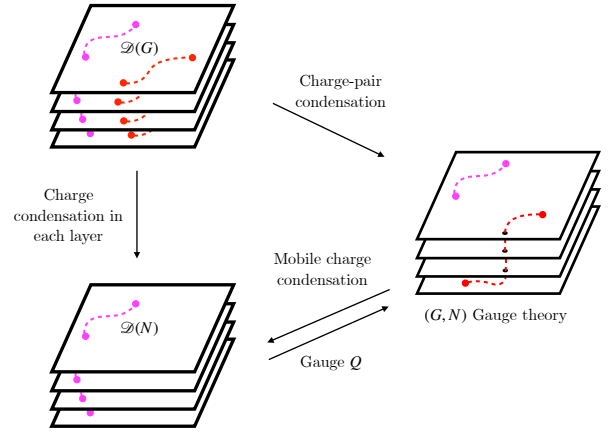


FIG. 2. The 1-foliated (G, N) gauge theory can be obtained from starting with a stack of $\mathcal{D}(N)$ models, and gauging a global Q symmetry enriching the theory. Alternatively, it can also be obtained by starting with a stack of $\mathcal{D}(G)$ models, and condensing pairs of charges (shown in red) in adjacent layers. The charge pairs that are condensed depend on the choice of N , and are exactly the charges that become mobile in the hybrid model. Fluxes are not drawn for simplicity.

The relation between the (G, N) gauge theory and stacks of familiar 2 + 1d topological phases is shown in Figure 2.

We note that, because the subsystem symmetry planes do not intersect, one can in fact choose N to be a non-abelian group. Therefore, the construction in this section holds generally for any finite group G .

Given the exact sequence Eq. (7) corresponding to the group extension, we place $\mathbb{C}[G]$ on each edge oriented in the x or y directions of the cubic lattice, equipped with left and right multiplication operators

$$L_e^g |g_e\rangle = |gg_e\rangle, \quad (9)$$

$$R_e^g |g_e\rangle = |g_e\bar{g}\rangle, \quad (10)$$

where $\bar{g} \equiv g^{-1}$. Furthermore, on each edge oriented in the z direction, we place $\mathbb{C}[Q]$ with operators

$$L_e^q |q_e\rangle = |qq_e\rangle, \quad (11)$$

$$R_e^q |q_e\rangle = |q_e\bar{q}\rangle, \quad (12)$$

Furthermore, for notational convenience, we define

$$q'_e = \begin{cases} \pi(g_e); & \text{if } e \text{ is in the } x \text{ or } y \text{ directions} \\ q_e; & \text{if } e \text{ is in the } z \text{ direction} \end{cases} \quad (13)$$

The Hamiltonian is given by

$$H_{(G,N)} = - \sum_v \mathbf{A}_v^G - \sum_{p_\perp} \mathbf{B}_{p_\perp} - \sum_{p_\parallel} \mathbf{B}_{p_\parallel}, \quad (14)$$

$$\mathbf{A}_v^G = \frac{1}{|G|} \sum_{g \in G} \mathbf{A}_v^g,$$

where p_{\parallel} denotes plaquettes in xy plane, and p_{\perp} denotes plaquettes in the xz and yz planes.

The explicit form of the operators are

$$\mathbf{A}_v^g = \begin{array}{c} | \\ \hline L^{\pi(g)} \\ \hline R^g \\ \hline L^g \\ \hline R^{\pi(g)} \\ \hline | \end{array} \quad (15)$$

$$\mathbf{B}_{p_{\perp}} = \delta_{1, q'_1 q'_2 \bar{q}'_3 \bar{q}'_4} \left| \begin{array}{cc} \xrightarrow{g_2} & \\ q_1 & q_3 \\ \xleftarrow{g_4} & \end{array} \right\rangle \left\langle \begin{array}{cc} \xrightarrow{g_2} & \\ q_1 & q_3 \\ \xleftarrow{g_4} & \end{array} \right| \quad (16)$$

$$\mathbf{B}_{p_{\parallel}} = \delta_{1, g_1 g_2 \bar{g}_3 \bar{g}_4} \left| \begin{array}{ccc} & \xrightarrow{g_1} & \\ g_4 & & g_2 \\ & \xleftarrow{g_3} & \end{array} \right\rangle \left\langle \begin{array}{ccc} & \xrightarrow{g_1} & \\ g_4 & & g_2 \\ & \xleftarrow{g_3} & \end{array} \right| \quad (17)$$

1. Excitations and fusion

As in the quantum double models, excitations of the hybrid model can be obtained by applying appropriate ribbon operators [3, 4]. For simplicity, we only discuss how to create pure charge and pure flux excitations.

Charge excitations are labeled by irreps μ of the G , and can be excited at the end points of a direct string L . First, let us assume the string is purely in a fixed xy plane denoted L_{xy} , consisting of an ordered set of edges e_1, e_2, \dots, e_n . Let $\Gamma^{\mu, G}$, be the matrix representation of the irrep μ of G , then for each $i, i' = 1 \dots d_{\mu}$, where d_{μ} is the dimension of the irrep μ , one can construct the following string operator

$$F_{L_{xy}}^{\mu, (i, i')} = \sum_{\{g_e\}} \Gamma_{i, i'}^{\mu, G} \left(g_{e_1}^{O_{e_1}} g_{e_2}^{O_{e_2}} \dots g_{e_n}^{O_{e_n}} \right) |\{g_e\}\rangle \langle\{g_e\}| \quad (18)$$

where $\{g_e\}$ are group elements along L_{xy} and O_e inverts the group element if the path of the string L_{xy} goes against the orientation of that edge. This ribbon violates \mathbf{A}_v only at the end points. Furthermore, under the operators \mathbf{A}_v^g , the left (right) end point transforms under the representation μ ($\bar{\mu}$) of G .

The above string operator seems to imply that all charge excitations are planons. However, that is not the case. As we have argued in Sec. III B, a charge corresponding to the irrep μ is actually mobile if μ can be pulled back from some irrep ν of Q . That is,

$$\Gamma^{\mu, G}(g) = \Gamma^{\nu, Q}(\pi(g)) \quad \forall g \in G \quad (19)$$

This can be seen explicitly by constructing the corresponding string operator. For a direct string L (not necessarily confined to a single xy plane), consider

$$F_L^{\mu, (i, i')} = \sum_{\{g_e, q_e\}} \Gamma_{i, i'}^{\nu, Q} \left(q_{e_1}^{O_{e_1}} q_{e_2}^{O_{e_2}} \dots q_{e_n}^{O_{e_n}} \right) |\{g_e, q_e\}\rangle \langle\{g_e, q_e\}|. \quad (20)$$

This operator also violates \mathbf{A}_v only at the end points of the string, and the left (right) end point transform as μ ($\bar{\mu}$) of G under \mathbf{A}_v^g . It is also apparent that by projecting \mathbf{A}_v^g to the subgroup Q , the end points transform under the irreps ν ($\bar{\nu}$) of Q . Finally, we remark that if L is in a fixed xy plane, the general string operator in (20) reduces to Eq. (18) defined in a single plane, by applying the definition of the pullback (19).

To complete the argument, we must show that the remaining irreps of G (i.e. the irreps μ for which Eq. (19) does not hold), once created, cannot move out of their respective planes. Intuitively, this is because such a charge, when moved outside its original plane, will violate the conservation law of the new plane it enters. Suppose that such an irrep μ were mobile. This means that we are able to move a single such charge freely into a new layer. Consider \mathbf{A}_v^g where g is restricted to the subgroup N . Since $\pi(g) = 1$, \mathbf{A}_v^g only acts on each xy plane, and therefore we see that $\prod_{\text{plane}} \mathbf{A}_v^g = 1$. However, the charge moved to this new layer must transform non-trivially under $\prod_{\text{plane}} \mathbf{A}_v^g$ and is therefore a contradiction.

To conclude, the charges fuse according to the fusion category $\text{Rep}(G)$, just as the quantum double model of G . The additional structure (reflecting the choice of N in the (G, N) gauge theory) is that certain charges are planons. As a result, we note that generally, such planons can fuse into a direct sum of other charges, some of which are mobile.

Now, we discuss a basis of which one can create general excitations of the hybrid model. Consider the following ribbon operator (identical to those in the quantum double model) which are labeled by two group elements g and l .

$$F^{g, l} \left| \begin{array}{cccc} & \xrightarrow{k_1} & \xrightarrow{k_2} & \dots \\ h_1 & & h_2 & h_3 \\ & \xleftarrow{h_1} & \xleftarrow{h_2} & \dots \end{array} \right\rangle \quad (21)$$

$$= \delta_{l, k_1 k_2 \dots} \left| \begin{array}{cccc} & \xrightarrow{k_1} & \xrightarrow{k_2} & \dots \\ g h_1 & & k_1 g k_1 h_2 & k_2 k_1 g k_1 k_2 h_3 \\ & \xleftarrow{h_1} & \xleftarrow{h_2} & \dots \end{array} \right\rangle$$

For $g = 1$, an appropriate superposition of $F^{1, l}$ (namely the Fourier transform) gives the string operator for the charge excitations Eq. (18).

Let us now consider $g \neq 1$. The type of excitation will depend on its conjugacy class. First, consider a group element g where $\pi(g) = 1$. We see that only two $\mathbf{B}_{p_{\parallel}}$ terms at the ends of the ribbon are violated. Importantly, all the $\mathbf{B}_{p_{\perp}}$ operators touching this ribbon are not violated since the modified group element on each edge is of the form $(\prod_i k_i) g (\prod_i k_i)$, which is the same conjugacy class as g . Therefore, they are also projected by π to 1. We therefore see that the resulting excitations are a pair of planons.

Next, consider the case where $\pi(g) \neq 1$. Using the same ribbon operator as above, we find that both $\mathbf{B}_{p_{\perp}}$ and $\mathbf{B}_{p_{\parallel}}$ are violated. Therefore, the resulting flux is a loop excitation. This loop excitation is fully mobile, as we can also bend the loop into the xy plane by left multiplying with $\pi(g)$ on z edges and appropriately conjugating $\pi(g)$ as we expand the loop.

Therefore, we have constructed flux excitations (violation of plaquette terms), whose type depends on the conjugacy class. In general, charge excitations can be created as well, forming either a dyon (bound state of charge and flux planons)

or a bound state of a point charge and a flux loop. Further analysis is required to find the proper basis for these excitations.

To conclude this section, we reinterpret the local Wilson operators as a product of closed trajectories of the charge and flux operators. The projector $B_{p\parallel}$ can be decomposed in terms of characters of G : $\chi^{\mu,G} = \text{Tr}(\Gamma^{\mu,G})$ since

$$\delta_{1,g_1g_2\bar{g}_3\bar{g}_4} = \frac{1}{|G|} \sum_{\mu} d_{\mu} \chi^{\mu,G}(g_1g_2\bar{g}_3\bar{g}_4) \quad (22)$$

Physically, each term in the sum denotes a closed loop of the gauge charge for each irrep μ . Similarly, $B_{p\perp}$ can be decomposed into characters of Q since

$$\delta_{1,q'_1q'_2\bar{q}'_3\bar{q}'_4} = \frac{1}{|Q|} \sum_{\nu} d_{\nu} \chi^{\nu,Q}(q'_1q'_2\bar{q}'_3\bar{q}'_4). \quad (23)$$

Here, we sum over irreps ν of Q , which in turn, can be pulled back to the mobile irreps of G . Therefore, each term in the sum denotes a closed loop of all the mobile charges.

V. 3-FOLIATED (G, N) GAUGE THEORY

In this section, we give the commuting projector Hamiltonian that realizes the 3-foliated (G, N) gauge theory. We first introduce the necessary terminology required to define the Hamiltonian in Sec. VA. Notably, we review the factor system corresponding to a group extension in Sec. VA 1. In Sec. VB, we derive this Hamiltonian by gauging a paramagnet with a particular mix of global and subsystem symmetries, which we call a 2-subsystem symmetry.

Our discussion here will focus on the case where the subsystem symmetry consists of three planes on a cubic lattice (generalizing the X-cube model[13]). Nevertheless it is straightforward to write down similar models with other subsystem symmetries, including those with fractal support as well.

A. The lattice model

Our model is defined on a cubic lattice with additional diagonal edges as shown in Figure 3. We place an N degree of freedom $\mathbb{C}[N]$ on each (square) plaquette and a $Q = G/N$ degree of freedom $\mathbb{C}[Q]$ on each edge of the lattice. The Hamiltonian takes the following form,

$$H = - \sum_v A_v^G - \sum_c \sum_{r=x,y,z} B_{c,r}^N - \sum_{\nabla} B_{\nabla}^Q, \quad (24)$$

where A_v^G , $B_{c,r}^N$ and B_{∇}^Q are commuting projectors defined on each vertex v , cube c , and triangle ∇ in the lattice, respectively.

The terms in the Hamiltonian are such that

1. When $N = \mathbb{Z}_1$, $B_{c,r}^N = \mathbb{1}$ and A_v^G and B_{∇}^Q are respectively the vertex and plaquette terms of the 3D quantum double model with gauge group $G = Q$.

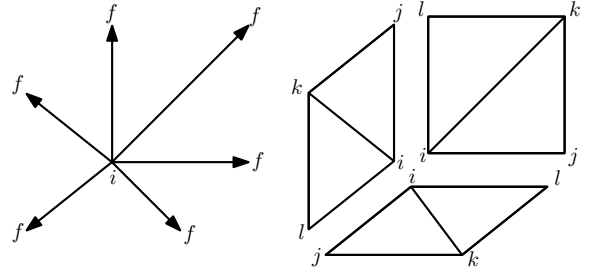


FIG. 3. **Description of the Lattice for the 3-foliated (G, N) gauge theory:** Diagonal edges are added to each plaquette in the cubic lattice. *Left:* each edge $e = (if)$ is oriented, pointing outward from an “initial” vertex i towards a “final” vertex f . *Right:* ordering of vertices for each square plaquette $p = (ijkl)$

2. When $Q = \mathbb{Z}_1$, $B_{\nabla}^Q = \mathbb{1}$ and A_v^G and $B_{c,r}^N$ are respectively the vertex and cube terms of the X-cube model with gauge group $G = N$.

It is helpful to describe qualitatively the aspects of this (G, N) gauge theory. The projectors B_{∇}^Q and $B_{c,r}^N$ are delta functions which enforces the gauge constraint (we only enforce them energetically in our Hamiltonian, but they can also be strictly enforced if needed). The vertex term can be decomposed as

$$A_v^G = \frac{1}{|G|} \sum_{g \in G} A_v^g. \quad (25)$$

By factoring a group element $g \in G$ into a pair (n, q) where $n \in N$ and $q \in Q$, the vertex term A_v^g can be thought of as the vertex term in the 3D Q quantum double model corresponding to the group element q , but dressed with controlled operators in such a way that the multiplication of A_v^g obeys the group law in G . That is, for $g, h \in G$,

$$A_v^g A_v^h = A_v^{gh} \quad (26)$$

There are various excitations in the model, either labeled by representations of the group G (charges) or conjugacy classes of G (fluxes) with different mobilities. They are measured by the violations of terms in this commuting projector Hamiltonian. First, charge excitations are violations of $A_v^G = 1$. From the group law above, it follows that charge excitations must transform as irreps of G . And non-abelian charges are those transform under higher-dimensional irreps of G . Furthermore, the model has the property that for group elements in the normal subgroup N , the product of vertex terms over individual planes is one

$$\prod_{v \in \text{plane}} A_v^g = 1, \quad \forall g \in \iota(N). \quad (27)$$

This conservation law implies that any excitation that transform non-trivially under the normal subgroup N must be a fracton. Otherwise, that excitation is fully mobile.

Second, the flux term B_{∇}^Q is the same as that of the Q quantum double model. A violation of this flux term represents a

mobile flux loop. Finally, $\mathbf{B}_{c,r}^N$ is a modified flux term of the X-cube model with gauge group N , whose violations are li-neon excitations.

In order to describe precisely the terms in the Hamiltonian, we will first review the necessary machinery. First, we review factor systems corresponding to group extensions, and define corresponding operators used to define the projectors in our Hamiltonian.

1. Factor systems

In the following, all groups are defined with the usual multiplication operation, 1 denotes the identity element, and the inverse of $g \in G$ is denoted \bar{g} .

Given a group G and an abelian normal subgroup $N \triangleleft G$, one has an exact sequence

$$1 \rightarrow N \xrightarrow{\iota} G \xrightarrow{\pi} Q \rightarrow 1 \quad (28)$$

where ι is injective and π is surjective. Such a group extension is determined by a factor system, which consists of two pieces of data

1. A map $\sigma : Q \rightarrow \text{Aut}(N)$. That is for each $q \in Q$, σ^q defines an automorphism on N .
2. A cocycle $\omega : Q^2 \rightarrow N$ which represents a cohomology class $[\omega] \in H_\sigma^2(Q, N)$.

Furthermore, we will also make the following assumptions, which for each factor system can always be chosen

1. σ^1 acts as the identity automorphism.
2. A canonical choice of ‘‘normalized’’ cocycles where $\omega(1, q) = \omega(q, 1) = 1$.

Let us now explain the group extension. Given a factor system, any $g \in G$ can be uniquely labeled as a pair $(n, q) \equiv {}^n q$ for some $n \in N$, and $q \in Q$. The group law is given by

$${}^{n_1} q_1 \cdot {}^{n_2} q_2 = \omega(q_1, q_2) {}^{n_1 \sigma^{q_1}[n_2]} q_1 q_2 \quad (29)$$

Here, associativity of group multiplication is guaranteed by the fact that ω satisfies the so-called cocycle condition

$$\sigma^{q_1}[\omega(q_2, q_3)] \bar{\omega}(q_1 q_2, q_3) \omega(q_1, q_2 q_3) \bar{\omega}(q_1, q_2) = 1. \quad (30)$$

Here, $\bar{\omega}$ is the inverse cocycle of ω .

The maps ι and π in the short exact sequence are given by

$$\iota(n) = {}^n 1 \quad (31)$$

$$\pi({}^n q) = q \quad (32)$$

So it is clear that $\pi \circ \iota = 1$, the identity element in Q . For convenience, we also define a map $t : G \rightarrow N$ as

$$t(g) = t({}^n q) \equiv n \quad (33)$$

so that we can express a group element g as

$$g = {}^n q = {}^{t(g)} \pi(g). \quad (34)$$

Note that unlike π , the map t is not a homomorphism.

The maps π and t satisfy the following useful identities which can be proven from the definitions. They will be useful for the gauging process.

$$\pi(gg_v) = qq_v \quad (35)$$

$$\pi(g_v \bar{g}) = q_v \bar{q} \quad (36)$$

$$t(gg_i \bar{g}_f) = \bar{\omega}(q, q_i \bar{q}_f) n \sigma^q[t(g_i \bar{g}_f)], \quad (37)$$

$$t(g_i \bar{g} \bar{g}_f) = t(g_i \bar{g}_f) \bar{\omega}(q_i \bar{q} \bar{q}_f, q) \sigma^{q_i \bar{q} \bar{q}_f}[\bar{n}], \quad (38)$$

$$t(g_i ({}^{n_1} \bar{g})_f) = \sigma^{q_i}[n] t(g_i \bar{g}_f). \quad (39)$$

2. Definition of operators

Next, we proceed to define operators in the Hilbert space of our model. We consider a cubic lattice with an additional diagonal edge added to each plaquette on the cubic lattice as shown in Fig. 3. We place the group algebra $\mathbb{C}[N]$ on each square plaquette of the cubic lattice, and $\mathbb{C}[Q]$ on each edge. First of all, we can define the usual left and right multiplication operators as in the quantum double model

$$L_p^n |n_p\rangle = |nn_p\rangle, \quad (40)$$

$$R_p^n |n_p\rangle = |n_p \bar{n}\rangle, \quad (41)$$

$$L_e^q |q_e\rangle = |qq_e\rangle, \quad (42)$$

$$R_e^q |q_e\rangle = |q_e \bar{q}\rangle, \quad (43)$$

which acts purely either on the N d.o.f. (each plaquette) or the Q d.o.f. (each edge). In addition, the factor system allows us to define additional operators. First, for a fixed $q \in Q$, we can define

$$\Sigma_p^q |n_p\rangle = |\sigma^q[n_p]\rangle \quad (44)$$

which applies the automorphism σ^q to n . Next, as a slight abuse of notation, we define

$$\Sigma_e^q [n] |q_e\rangle = \sigma^{q_e}[n] |q_e\rangle \quad (45)$$

$$\Omega(e, q) |q_e\rangle = \omega(q_e, q) |q_e\rangle \quad (46)$$

$$\Omega(q, e) |q_e\rangle = \omega(q, q_e) |q_e\rangle \quad (47)$$

which for a fixed n or q reads off the Q d.o.f. q_e on edge e and constructs N group elements $\sigma^{q_e}[n]$, $\omega(q_e, q)$, or $\omega(q, q_e)$. The above are not operators per se, but can be used to define controlled operators with Q d.o.f. as the control site and N d.o.f. as the target site by combining them with left and right multiplication. For example, the operator $L_p^{\Sigma_e[n]}$ is defined as

$$L_p^{\Sigma_e[n]} |n_p, q_e\rangle = L_p^{\sigma^{q_e}[n]} |n_p, q_e\rangle = |\sigma^{q_e}[n] n_p, q_e\rangle \quad (48)$$

which reads the Q d.o.f. on site e , q_e , permutes n by σ^{q_e} then left multiplies the result to the plaquette p . For completion, we define the operators used in the paper according to this notation

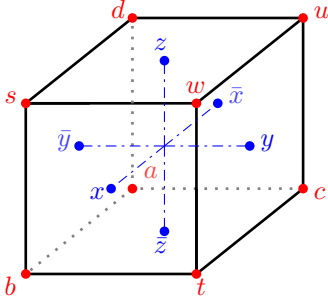


FIG. 4. Label for the vertices (red) and faces (blue) for each cube used to define the projector $B_{c,r}^N$.

$$R_p^{\Sigma^e[n]} |n_p, q_e\rangle = R_p^{\sigma^{q_e}} |n_p, q_e\rangle = |n_p \sigma^{q_e} [\bar{n}], q_e\rangle \quad (49)$$

$$L_p^{\Omega(e,q)} |n_p, q_e\rangle = L_p^{\omega(q_e,q)} |n_p, q_e\rangle = |\omega(q_e, q) n_p, q_e\rangle \quad (50)$$

$$R_p^{\Omega(e,q)} |n_p, q_e\rangle = R_p^{\omega(q_e,q)} |n_p, q_e\rangle = |n_p \bar{\omega}(q_e, q), q_e\rangle \quad (51)$$

$$L_p^{\Omega(q,e)} |n_p, q_e\rangle = L_p^{\omega(q,q_e)} |n_p, q_e\rangle = |\omega(q, q_e) n_p, q_e\rangle \quad (52)$$

$$R_p^{\Omega(q,e)} |n_p, q_e\rangle = R_p^{\omega(q,q_e)} |n_p, q_e\rangle = |n_p \bar{\omega}(q, q_e), q_e\rangle \quad (53)$$

Lastly, we define the following controlled operator

$$\Sigma_p^e |n_p, q_e\rangle = |\sigma^{q_e} [n_p], q_e\rangle \quad (54)$$

which reads off q_e and applies the corresponding permutation $\sigma_e^{q_e}$ to n_p .

3. Definition of projectors

Having defined the operators, we can now define our model. First, we define a local ordering of the vertices to each edge $e = (if)$ and each square plaquette $p = (ijkl)$ as shown in Fig. 3, and denote $e \rightarrow v$ ($e \leftarrow v$) as incoming (outgoing) edges towards (from) the vertex v . The projectors are given by

$$A_v^G = \sum_{g \in G} A_v^g \quad (55)$$

$$A_v^g = \prod_{p|v=j,l} R_p^{\Omega((iv),q)\Sigma^{(iv)}[n]} \times \prod_{p|v=k} L_p^{\Omega((iv),q)\Sigma^{(iv)}[n]} \times \prod_{e \leftarrow v} R_e^q \prod_{e \rightarrow v} L_e^q \times \prod_{p|v=i} L_p^{\bar{\Omega}(q,(vj))\Omega(q,(vk))\bar{\Omega}(q,(vl))n\Sigma_p^q}, \quad (56)$$

$$B_{\nabla}^Q = \sum_{\{q\}} \delta_{1,q_{ad}q_{du}q_{au}} |\{q\}\rangle \langle \{q\}|, \quad ; \nabla = (adu) \quad (57)$$

$$B_{c,x}^N = \sum_{\{n,q\}} \delta_{1,\omega(q_{ad},q_{ds})\bar{\omega}(q_{ad},q_{dw})\omega(q_{ad},q_{du})\bar{\omega}(q_{ac},q_{ct})\omega(q_{ac},q_{cw})\bar{\omega}(q_{ac},q_{cu})\sigma^{q_{ac}}[n_y]\sigma^{q_{ad}}[\bar{n}_z]\bar{n}_y n_x} |\{n,q\}\rangle \langle \{n,q\}| \quad (58)$$

$$B_{c,y}^N = \sum_{\{n,q\}} \delta_{1,\omega(q_{ab},q_{bt})\bar{\omega}(q_{ab},q_{bw})\omega(q_{ab},q_{bs})\bar{\omega}(q_{ad},q_{du})\omega(q_{ad},q_{dw})\bar{\omega}(q_{ad},q_{ds})\sigma^{q_{ad}}[n_z]\sigma^{q_{ab}}[\bar{n}_x]\bar{n}_z n_x} |\{n,q\}\rangle \langle \{n,q\}| \quad (59)$$

$$B_{c,z}^N = \sum_{\{n,q\}} \delta_{1,\omega(q_{ac},q_{cu})\bar{\omega}(q_{ac},q_{cw})\omega(q_{ac},q_{ct})\bar{\omega}(q_{ab},q_{bs})\omega(q_{ab},q_{bw})\bar{\omega}(q_{ab},q_{bu})\sigma^{q_{ab}}[n_x]\sigma^{q_{ac}}[\bar{n}_y]\bar{n}_x n_y} |\{n,q\}\rangle \langle \{n,q\}| \quad (60)$$

Here, the edges used to define the $B_{c,r}^N$ operators are those connecting two vertices as labeled in Figure 4. We further note that the three $B_{c,r}^N$ operators are just C_3 rotations of each other, which is achieved via cyclically permuting the vertices b, c, d , vertices s, t, u , plaquettes x, y, z , and plaquettes $\bar{x}, \bar{y}, \bar{z}$.

With the explicit expressions, let us verify the claims made earlier

1. When $N = \mathbb{Z}_1$, the only elements of N are 1 and so $B_{c,r}^N = \mathbb{1}$. The vertex term reduces to

$$A_v^g = \frac{1}{|G|} \prod_{e \leftarrow v} R_e^g \prod_{e \rightarrow v} L_e^g \quad (61)$$

which is just the vertex term of the 3D quantum double model with gauge group $G = Q$.

2. When $Q = \mathbb{Z}_1$, $B_{\nabla}^Q = \mathbb{1}$. The vertex and cube terms reduce to

$$A_v^g = \prod_{p|v=j,l} R_p^n \times \prod_{p|v=i,k} L_p^n \quad (62)$$

$$B_{c,x}^N = \sum_{\{n\}} \delta_{1,n_y \bar{n}_z \bar{n}_y n_x} |\{n\}\rangle \langle \{n\}| \quad (63)$$

$$B_{c,y}^N = \sum_{\{n\}} \delta_{1,n_z \bar{n}_x \bar{n}_z n_x} |\{n\}\rangle \langle \{n\}| \quad (64)$$

$$B_{c,z}^N = \sum_{\{n\}} \delta_{1,n_x \bar{n}_y \bar{n}_x n_y} |\{n\}\rangle \langle \{n\}| \quad (65)$$

which are those of the X-cube model with gauge group $G = N$.

Let us now analyze the terms of the Hamiltonian in more detail. First, consider the vertex term A_v^g . When restricted to the subgroup N (i.e. those of the form $g = {}^n 1$), the vertex term A_v^g is that of the X-cube model with gauge group N . Furthermore, when restricted to group elements g of the form $g = {}^1 q$, the vertex term A_v^g can be interpreted as the vertex term of the Q quantum double model dressed with certain combinations of controlled operators. These operators guarantee the correct group multiplication of A_v^g as given in Eq. (26).

Moving on to the flux terms, the plaquette term B_{∇}^Q is the same as that in the Q quantum double model. A violation of this plaquette represents a mobile flux loop labeled by a conjugacy class of G whose image under π is a non-trivial conjugacy class of Q . The cube term $B_{c,r}^N$ is a modified flux term of the X-cube model with gauge group N . Violations of such terms are lineons labeled by the remaining conjugacy classes of G .

B. Derivation of the 3-foliated (G, N) gauge theory

In this section, we provide a derivation of the 3-foliated (G, N) gauge theory. We will start by introducing a paramagnet with a 2-subsystem symmetry, which we will rigorously define. Then, we will proceed to gauge the 2-subsystem symmetry, which can be done in two steps. First, we gauge the N subsystem symmetry, which is a normal subgroup of (G, N) to obtain an X-cube model with gauge group N enriched by a global symmetry $Q = G/N$. Then, we will gauge Q to obtain the (G, N) gauge theory. The equivalent gauging procedure for the quantum double model is reviewed in detail in Appendix A.

1. 2-Subsystem Symmetry

We will begin with a proper definition of a 2-subsystem symmetry. A brief discussion of abelian 2-subsystem symmetries has been presented in Ref. 1.

A 2-subsystem symmetry can be defined given the following data

1. A global symmetry group G
2. A normal subgroup $N \triangleleft G$
3. The type of region on which N acts as a subsystem symmetry (e.g. 1-foliated, 3-foliated, fractal,...)

Note that first two data is equivalent to specifying N, Q and the factor system σ and ω .

If we ignore the geometrical input of the type of subsystem symmetry, then (G, N) is a group given uniquely by the group extension

$$1 \rightarrow N^L \rightarrow (G, N) \rightarrow Q \rightarrow 1 \quad (66)$$

where $N^L \equiv N_1 \times \cdots \times N_L$ is a product of L identical copies of N , which represents the number of independent subsystem symmetries. The group extension above can be specified by the map $\sigma' : Q \rightarrow \text{Aut}(N^L)$ which acts as σ identically on all copies of N in N^L , and a representative cocycle ω' of $H^2(Q, N^L)$ chosen to be $\omega' = \prod_{l=1}^L \iota_l \circ \omega$ where $\iota_l : N \rightarrow N^L$ is the embedding of N to the l^{th} copy of N^L .

The 2-subsystem symmetry can be realized as the following on a lattice model. First, we define the local Hilbert space on each vertex of the lattice to be the group algebra $\mathbb{C}[G]$, whose basis vectors are denoted $|g\rangle$ for $g \in G$. The onsite symmetry action of G acts via right multiplication

$$R_v^g : |h_v\rangle \rightarrow |h_v g\rangle \quad (67)$$

The 2-subsystem symmetry can now be defined as

$$\begin{aligned} \text{Global symmetry } G: & \prod_v R_v^g \\ \text{Subsystem symmetry } N: & \prod_{v \in \text{sub}} R_v^n \end{aligned} \quad (68)$$

Here, ‘‘sub’’ is a subregion specified by the geometric input of the subsystem symmetry.

In passing, we would like to make a comparison to 2-group symmetries[40–43], which can be thought of as a particular extension of global (0-form) symmetries by 1-form symmetries (and whose name we were inspired from). In particular, one could ask why we expect the input data for 2-subsystem symmetry to depend on a 2-cocycle rather than a 3-cocycle as in 2-groups. Here, we will give a physically motivated answer from the perspective of fractionalization. Recall that in 2D, gauging a normal subgroup N of a paramagnet with G symmetry, results in an N topological order where the symmetry fractionalization on the charge anyons are determined by a cohomology class $H_\sigma^2(Q, N)$, which determines the group extension[44–46]. Similarly, for 2-groups, after gauging the 1-form symmetry N the resulting abelian topological order is an SET where the remaining 0-form global symmetry Q fractionalizes on the loop excitations according to the cohomology class $H_\sigma^3(Q, N)$.⁹ A way to interpret the different fractionalization classes is to view the corresponding string/membrane operators of the anyons or loop excitations as attached with different 1d or 2d ‘‘ N valued SPTs protected by Q ’’. In this way, the fractionalization can be interpreted as an anomaly coming from the boundary of the attached SPT phase [48].

Returning to the case for 2-subsystem symmetry, after gauging the subsystem symmetry N , the gauge charges are fractons, which are 0-dimensional. Therefore, the fractionalization class should be thought of as the end points of a 1D SPT, and therefore it is reasonable to expect that this is captured via a 2-cocycle in $H_\sigma^2(Q, N)$.

⁹ for an explicit lattice calculation, see for example Ref. 47.

2. 2-subsystem paramagnet

To begin the derivation, we will start with a cubic lattice where each vertex is $\mathbb{C}[G]$. In addition to the paramagnetic term, we will write down additional kinetic terms that respects the 2-subsystem symmetry.

On a cubic lattice with extra diagonal edges as shown in Fig. 3, we place the group algebra $\mathbb{C}[G]$ on each vertex. The Hamiltonian we will consider is

$$H = - \sum_v L_v - h_E \sum_e \Delta_e - h_P \sum_p \Delta_p, \quad (69)$$

which consists of the paramagnetic term and two types of kinetic terms Δ . For each edge $e = (if)$ and plaquette $p = (ijkl)$, we define

$$\begin{aligned} \Delta_e &= \sum_{q_i, q_f} \delta_{1, q_i \bar{q}_f} |q_i, q_f\rangle \langle q_i, q_f|. \quad (70) \\ \Delta_p &= \sum_{g_i, g_j, g_k, g_l} \delta_{1, t(g_i \bar{g}_j) \overline{t(g_i \bar{g}_k)} t(g_i \bar{g}_l)} \\ &\quad |g_i, g_j, g_k, g_l\rangle \langle g_i, g_j, g_k, g_l| \quad (71) \end{aligned}$$

where t is defined in Eq. (33). It is apparent that Δ_e commutes with the 2-subsystem symmetry Eq. (68), and we can see that Δ_p commutes with the global G symmetry, since right multiplication on all sites leaves terms of the form $t(g_i \bar{g}_j)$ invariant. Therefore, we only need to check that Δ_p commutes with the N planar symmetry. As an example, let us consider the case where the planar symmetry acts only on sites i and j of the plaquette p . $t(g_i \bar{g}_j)$ is invariant, and using Eq. (39), we see that the contributions coming from $\overline{t(g_i \bar{g}_k)}$ and $t(g_i \bar{g}_l)$ are respectively $\sigma^{q_i} [\bar{n}]$ and $\sigma^{q_i} [n]$, which cancel. Similarly, one can confirm that Δ_p is also invariant when the symmetry acts only on sites j and k , k and l , or l and i . Therefore, our Hamiltonian commutes with the 2-subsystem symmetry.

There are some remarks to be made about our Hamiltonian. First, the Hamiltonian does not have a planar symmetry for the full group G , which avoids the problem of having an additional local symmetry at each site given by the commutator subgroup $[G, G]$ when G is non-abelian. To see this, we note that the edge Ising term Δ_e does not commute with a planar symmetry g unless it is of the form $g = {}^n 1$. This is because for a given plane, one can consider an edge normal to the plane such that the symmetry acts on only one site of Δ_e (say site i_e). In such case, the delta function will transform as

$$\delta_{1, q_i \bar{q}_f} \rightarrow \delta_{1, q_i \bar{q}_f} \quad (72)$$

which is not invariant. Second, the constraint in the delta function for Δ_p is not equal to $t(g_i \bar{g}_j g_k \bar{g}_l)$. In fact, one can check that such a term does not commute with the 2-subsystem symmetry. Lastly, the Hamiltonian has additional symmetries coming from left multiplication, but they will not be important for our discussion, as we will gauge only the right multiplication symmetries.

3. Gauging N planar symmetries

We will now gauge the N planar symmetries (acting via right multiplication), and argue that we obtain a Symmetry-Enriched Fracton (SEF) order, where the fracton model is in the same phase as the X-cube model with gauge group N , but is enriched by a global symmetry Q . We demonstrate the permutation and fractionalization of the excitations of the SEF in Appendix C 2.

To gauge the N planar symmetries, we define the following ‘‘gauging map’’, which projects each vertex to a Q d.o.f. via π and maps the expression in the delta function of Δ_p to an N -plaquette d.o.f.. That is, for the four vertices surrounding a plaquette p , we map

$$\begin{array}{ccc} g_l & \text{---} & g_k \\ | & & | \\ g_i & \text{---} & g_j \end{array} \rightarrow \begin{array}{ccc} q_l & \text{---} & q_k \\ | & & | \\ q_i & \text{---} & q_j \end{array} \quad (73)$$

where

$$n_p = t(g_i \bar{g}_j) \overline{t(g_i \bar{g}_k)} t(g_i \bar{g}_l) \quad (74)$$

Note that the expression of n_p is just the constraint in the kinetic term Eq. (71). The reason this map can be thought of as gauging the planar symmetries because n_p is invariant under the planar symmetry action. Therefore, after the mapping only the global symmetry $Q = G/N$ is left as a physical symmetry acting on the system.

Let us work out how the operators are mapped. The Ising term Δ_e is unchanged, while Δ_p gets mapped to $T_p^1 \equiv |1\rangle \langle 1|_p$. Next, we must compute how L_v^g maps. For each plaquette p whose corner contains v , we identify whether v constitutes as the vertex i, j, k , or l of that plaquette. If $v = i$, then using Eq. (37), we see that under the action of L_v^g ,

$$L_v^g |n_p\rangle = |\bar{\omega}(q, q_i \bar{q}_j) \omega(q, q_i \bar{q}_k) \bar{\omega}(q, q_i \bar{q}_l) n \sigma^q [n_p]\rangle \quad (75)$$

Using Eq. (38), for $v = k$ we find

$$L_v^g |n_p\rangle = |\omega(q, q_i \bar{q}_k, q) \sigma^{q_i q \bar{q}_k} [n] n_p\rangle \quad (76)$$

while for $v = j, l$ we find

$$L_v^g |n_p\rangle = |n_p \bar{\omega}(q, q_i \bar{q}_k, q) \sigma^{q_i q \bar{q}_k} [\bar{n}]\rangle \quad (77)$$

Therefore, we conclude that

$$\begin{aligned} L_v^g \rightarrow A_v^g &= \prod_{p|v=j,l} R_p^{\Omega(i\bar{v}, q) \Sigma^{i\bar{v}} [n]} \times \prod_{p|v=k} L_p^{\Omega(i\bar{v}, q) \Sigma^{i\bar{v}} [n]} \\ &\quad \times L_v^g \times \prod_{p|v=i} L_p^{\Omega(q, v\bar{j}) \Omega(q, v\bar{k}) \Omega(q, v\bar{l}) n \Sigma_p^q}. \quad (78) \end{aligned}$$

where in the above we have defined

$$\Sigma^{i\bar{v}} [n] |q_i, q_v\rangle = \sigma_p^{q_i \bar{q}_v} [n] |q_i, q_v\rangle, \quad (79)$$

$$\Omega(i\bar{v}, q) |q_i, q_v\rangle = \omega(q, q_i \bar{q}_v, q) |q_i, q_v\rangle, \quad (80)$$

$$\Omega(q, v\bar{i}) |q_i, q_v\rangle = \omega(q, q_v \bar{q}_i) |q_i, q_v\rangle. \quad (81)$$

Finally, we impose the constraint which arises from gauging. Consider a cube with plaquettes and vertices depicted in Figure 4. We notice that for each plaquette p , if we define

$$\begin{aligned}\tilde{n}_p &= \sigma^{\bar{q}_i} [\omega(q_i \bar{q}_j, q_j) \bar{\omega}(q_i \bar{q}_k, q_k) \omega(q_i \bar{q}_l, q_l) n_p] \\ &= \sigma^{\bar{q}_i} [n_i] \sigma^{\bar{q}_j} [\bar{n}_j] \sigma^{\bar{q}_k} [n_k] \sigma^{\bar{q}_l} [\bar{n}_l],\end{aligned}\quad (82)$$

then we see that the following product of \tilde{n}_p over four plaquettes around a cube is the identity.

$$\tilde{n}_y \bar{\tilde{n}}_z \bar{\tilde{n}}_{\bar{y}} n_{\bar{z}} = 1 \quad (83)$$

Therefore, we can impose the following constraint energetically via

$$B_{c,x}^N = \sum_{\{n,q\}} \delta_{1, \bar{n}_y \bar{\tilde{n}}_z \bar{\tilde{n}}_{\bar{y}} n_{\bar{z}}} |\{n, q\}\rangle \langle \{n, q\}| \quad (84)$$

$$B_{c,y}^N = \sum_{\{n,q\}} \delta_{1, \bar{n}_x \bar{\tilde{n}}_z \bar{\tilde{n}}_{\bar{x}} n_{\bar{z}}} |\{n, q\}\rangle \langle \{n, q\}| \quad (85)$$

$$B_{c,z}^N = \sum_{\{n,q\}} \delta_{1, \bar{n}_x \bar{\tilde{n}}_y \bar{\tilde{n}}_{\bar{x}} n_{\bar{y}}} |\{n, q\}\rangle \langle \{n, q\}| \quad (86)$$

To conclude, the symmetry-enriched fracton Hamiltonian

takes the form

$$\begin{aligned}H_{\text{SEF}} &= -\frac{1}{|G|} \sum_v \sum_{g \in G} A_v^g - \sum_c \sum_{r=x,y,z} B_{c,r}^N \\ &\quad - h_E \sum_e \Delta_e - h_P \sum_p T_p^1,\end{aligned}\quad (87)$$

where the star term A_v^g term is given in eqn. (78), $B_{c,r}^N$ is given in eqn. (86). The Hamiltonian is exactly solvable in the limit $h_E = h_P = 0$.

In Appendix C 2, we perform a basis transformation that turns the N -d.o.f. on each plaquette from n_p to \tilde{n}_p in Eq. (82). In this basis, the N -d.o.f. forms the X-cube model with gauge group N , and we explicitly demonstrate the symmetry enrichment via the permutation/fractionalization of the excitations.

4. Gauging global Q symmetry

We now gauge the global Q symmetry acting by right multiplication via the gauging map $q_i \bar{q}_f \rightarrow q_e = q_{(if)}$. This maps $\Delta_e \rightarrow T_e^1 = |1\rangle \langle 1|_e$. For the vertex term, we obtain

$$A_v^g \rightarrow \mathbf{A}_v^g = \prod_{p|v=j,l} R_p^{\Omega((iv),q)\Sigma^{(iv)}[n]} \times \prod_{p|v=k} L_p^{\Omega((iv),q)\Sigma^{(iv)}[n]} \times \prod_{e \leftarrow v} R_e^q \prod_{e \rightarrow v} L_e^q \times \prod_{p|v=i} L_p^{\Omega(q,(vj))\Omega(q,(vk))\Omega(q,(vl))n} \Sigma_p^q. \quad (88)$$

To gauge $B_{c,x}^N$. We need to first write it explicitly in terms of n and q . Starting from Eq. (86), we can substitute the explicit expression of \tilde{n}_p in Eq. (82) and use the cocycle conditions to simplify. The resulting expression is

$$B_{c,x}^N = \sum_{\{n,q\}} \delta_{1, \omega(q_a \bar{q}_d, q_d \bar{q}_s) \bar{\omega}(q_a \bar{q}_d, q_d \bar{q}_w) \omega(q_a \bar{q}_d, q_d \bar{q}_u) \bar{\omega}(q_a \bar{q}_c, q_c \bar{q}_t) \omega(q_a \bar{q}_c, q_c \bar{q}_w) \bar{\omega}(q_a \bar{q}_c, q_c \bar{q}_u) \sigma^{q_a \bar{q}_c} [n_y] \sigma^{q_a \bar{q}_d} [\bar{n}_z] \bar{n}_{\bar{y}} n_{\bar{z}}} |\{n, q\}\rangle \langle \{n, q\}| \quad (89)$$

Therefore, we can now gauge this to

$$B_{c,x}^N \rightarrow \mathbf{B}_{c,x}^N = \sum_{\{n,q\}} \delta_{1, \omega(q_{ad}, q_{ds}) \bar{\omega}(q_{ad}, q_{dw}) \omega(q_{ad}, q_{du}) \bar{\omega}(q_{ac}, q_{ct}) \omega(q_{ac}, q_{cw}) \bar{\omega}(q_{ac}, q_{cu}) \sigma^{q_{ac}} [n_y] \sigma^{q_{ad}} [\bar{n}_z] \bar{n}_{\bar{y}} n_{\bar{z}}} |\{n, q\}\rangle \langle \{n, q\}| \quad (90)$$

The expression for $\mathbf{B}_{c,y}^N$ and $\mathbf{B}_{c,z}^N$ are similarly obtained or by performing a C_3 rotation around the $(1, 1, 1)$ axis, which simultaneously permutes vertices b, c, d and s, t, u , as well as faces x, y, z and faces $\bar{x}, \bar{y}, \bar{z}$.

In addition, we also impose a fluxless condition for every closed triangle ∇ . For example, for the triangle $\nabla = (adu)$ in Figure 4, we have

$$\mathbf{B}_{\nabla}^Q = \sum_{\{q\}} \delta_{1, q_{ad} q_{du} \bar{q}_{au}} |\{q\}\rangle \langle \{q\}| \quad (91)$$

To conclude the desired (G, N) gauge theory can be obtained by setting the transverse fields $h_E = h_P = 0$, which is the Hamiltonian (24).

The duality of the operators are summarized in Table V. In Appendix D we present various examples.

VI. DISCUSSION

We have systematically studied hybrid fracton orders that emerge from (G, N) gauge theories, in which the G global symmetry and N subsystem symmetries of a trivial, short-range-entangled quantum system are gauged. We conclude by discussing some open questions (see also the discussion in Ref. 1).

“Topological data” in Hybrid Fracton Phases: It remains an open question to completely characterize the topological

TABLE V. Mapping of operators in the (G, N) paramagnet, the SEF (N -X-cube order enriched by Q), and the (G, N) gauge theory. The definitions of these operators are summarized in Sec. V A 2.

(G, N) -Ising	SEF	(G, N) gauge theory
L_v^g	$A_v^g = \prod_{p v=j,l} R_p^{\Omega(i\bar{v},q)\Sigma^{i\bar{v}}[n]} \times \prod_{p v=k} L_p^{\Omega(i\bar{v},q)\Sigma^{i\bar{v}}[n]} \times L_v^q \times \prod_{p v=i} L_p^{\bar{\Omega}(q,v\bar{j})\Omega(q,v\bar{k})\bar{\Omega}(q,v\bar{l})n\Sigma_p^q}$	$A_v^g = \prod_{p v=j,l} R_p^{\Omega((iv),q)\Sigma^{(iv)}[n]} \times \prod_{p v=k} L_p^{\Omega((iv),q)\Sigma^{(iv)}[n]} \times \prod_{e \leftarrow v} R_e^q \times \prod_{e \rightarrow v} L_e^q \times \prod_{p v=i} L_p^{\bar{\Omega}(q,(vj))\Omega(q,(vk))\bar{\Omega}(q,(vl))n\Sigma_p^q}$
Δ_e	Δ_e	T_e^{-1}
Δ_p	T_p^{-1}	T_p^{-1}
1	$B_{c,x}^N = \sum_{\{n,q\}} \delta_{1,\bar{n}_y\bar{n}_z} \bar{n}_{\bar{y}}\bar{n}_{\bar{z}} \{n,q\}\rangle \langle\{n,q\} $	$B_{c,x}^N = \sum_{\{n,q\}} \delta_{1,\omega(q_{ad},q_{ds})\bar{\omega}(q_{ad},q_{du})\omega(q_{ad},q_{du})\bar{\omega}(q_{ac},q_{ct})\omega(q_{ac},q_{cu})\bar{\omega}(q_{ac},q_{cu})\sigma^{q_{ac}}[n_y]\sigma^{q_{ad}}[\bar{n}_z]\bar{n}_{\bar{y}}\bar{n}_{\bar{z}} \{n,q\}\rangle \langle\{n,q\} $
1	1	$B_{\nabla}^Q = \sum_{\{q\}} \delta_{1,q_{ad}q_{du}\bar{q}_{au}} \{q\}\rangle \langle\{q\} $
$\prod_{v \in \text{plane}} R_v^n$	1	1
$\prod_v R_v^g$	$\prod_v R_v^q$	1

data of the excitations in the non-Abelian hybrid orders presented here, similar to the data in 3D quantum double models [6, 49–52]. This data includes the quantum dimensions of the non-Abelian excitations, and their fusion and braiding. It is also interesting to study the three-loop braiding statistics [49, 50, 53–61] for hybrid orders and other exotic processes involving a mix of mobile and restricted excitations. One could perhaps gain insight from the elementary excitations of 3D quantum double models, including their fusion and braiding properties.

Non-Abelian Fractons Beyond (G, N) Gauge Theory: We pointed out that as an intermediate step of gauging the N subsystem symmetry, we obtained a fracton model enriched by a global symmetry Q . An obvious generalization is to stack a Q -SPT before gauging the global symmetry, which would correspond to considering different possible defectification classes $H^4(Q, U(1))$ of the Q defect loops. This stacking could give rise to interesting hybrid models beyond the current construction. It also remains to be shown whether it is possible to obtain non-abelian fractons that transform under a group G that cannot arise from a group extension, such as the group A_5 . Another potential direction is whether the construction be generalized to beyond groups. For example, whether there are 3-foliated hybrid fracton orders where the description of the fusion and braiding data calls for more general categories as input.

Continuous groups: It would be interesting to construct the analog of (G, N) gauge theories where G is continuous, and study the properties of the resulting (presumably gapless) order. An initiative has begun in this direction using a field theoretical approach in Refs. 30–32, where we believe the corresponding 2-subsystem symmetry is $(O(2), U(1))$.

Note Added: While this paper was in preparation, we recently learnt of a work by Tu & Chang[36]), which also constructs similar models with non-abelian fractons by gauging a semidirect product of global and subsystem symmetries. The models they consider correspond to the specific case of a split

group extension in our work, and can be labeled as (S_3, \mathbb{Z}_3) and (D_4, \mathbb{Z}_2^2) 3-foliated gauge theories in our terminology.

ACKNOWLEDGMENTS

The authors are grateful to Yu-An Chen and Tyler Ellison for very helpful discussions on symmetry fractionalization and to Ashvin Vishwanath and Yuhui Zhang for interesting discussions on realizing fracton models from condensations. The authors thank David Aasen, Kevin Slagle, Ho Tat Lam, Shu-Heng Shao, and Cenke Xu for stimulating discussions. NT is supported by NSERC. WJ is supported by the Simons Foundation. This work was also partially supported by the Simons Collaboration on Ultra-Quantum Matter, which is a grant from the Simons Foundation.

Appendix A: Review of Gauging and the Quantum Double model

In this Appendix, we review the quantum double model of a group G denoted $\mathcal{D}(G)$ and the process of gauging. We first derive the model by gauging a paramagnet with G symmetry in A 1. In A 2 - A 4, we describe an alternative two-step gauging process. First, we “decompose” G into a normal subgroup N and its quotient group Q using the factor system of the corresponding group extension in Section V A 1. In A 3 we gauge the N global symmetry to obtain an N -topological order enriched by the quotient group Q . Finally, in A 4 we further gauge Q to recover a similar model which has an identical ground state to $\mathcal{D}(G)$. As an aside, C 1 demonstrates symmetry permutation and fractionalization of the SET obtained as an intermediate step from A 3 for some basic groups.

To setup some terminology, we will work with a directed graph, and define $e \rightarrow v$ and $e \leftarrow v$ to denote the set of all edges that enter and exit a vertex v , respectively. For each

edge e , we define i_e and f_e to be the initial and final vertices of each edge, respectively. When it is clear from context, the subscript e might be dropped. O_e denotes the orientation of each edge with respect to a clockwise loop going around each plaquette. Finally, we define a G degree of freedom (d.o.f) to mean a local Hilbert space $\mathbb{C}[G]$, which is situated of either the vertex or edge of the graph. The basis of each G d.o.f. is denoted by group elements $|g\rangle$ for each $g \in G$, where we will represent the identity element of G as 1 to not overlap with the symbol for the edge e . We will also note the inverse of g by \bar{g} .

1. $\mathcal{D}(G)$ from gauging G

The quantum double model of a group G is defined on an arbitrary directed graph. For simplicity, we will specialize to a square lattice in 2D with G d.o.f. on each edge e .

First define left and right multiplication operators

$$L_e^g |h_e\rangle = |gh_e\rangle \quad R^g |h_e\rangle = |h_e\bar{g}\rangle \quad (\text{A1})$$

and the projector to a group element g

$$T_e^g |h_e\rangle = \delta_{g,h_e} |h_e\rangle \quad (\text{A2})$$

The quantum double Hamiltonian under a transverse field is given by

$$H_{\mathcal{D}(G)} = - \sum_v \mathbf{A}_v - h_E \sum_e T_e^1 - \sum_p \mathbf{B}_p \quad (\text{A3})$$

where for each vertex v and plaquette p , we define commuting projectors

$$\mathbf{A}_v = \frac{1}{|G|} \sum_{g \in G} \left(\prod_{e \rightarrow v} R_e^g \right) \left(\prod_{e \leftarrow v} L_e^g \right) \quad (\text{A4})$$

$$\mathbf{B}_p = \sum_{e \subset p} \delta_{1, \prod_e g_e^{O_e}} |\{g_e\}\rangle \langle \{g_e\}| \quad (\text{A5})$$

and h_E is the strength of the transverse field. Physically, \mathbf{A}_v enforces a no-charge condition on the ground state, while \mathbf{B}_p enforces a no-flux condition via the delta function.

We will now derive the quantum double model by starting with a lattice model of ‘‘matter’’ fields with a global G symmetry, then gauging the G symmetry. Here, we will opt to use a Kramers-Wannier duality to perform the gauging. In Appendix B, we alternatively perform the gauging by minimally coupling the model to a G gauge field [5, 7] and show that it produces the same result.

Using the same graph as before, we will start out with a different Hilbert space. We place G -degrees of freedom on each vertex of the graph. The Hamiltonian is a generalization of the Ising model to G -variables

$$H = - \sum_v L_v - h_E \sum_e \Delta_e, \quad (\text{A6})$$

where

$$L_v = \frac{1}{|G|} \sum_{g \in G} L_v^g = |+\rangle \langle +| \quad (\text{A7})$$

$$\Delta_e = \sum_{g_i, g_f} \delta_{1, g_i \bar{g}_f} |g_i, g_f\rangle \langle g_i, g_f|. \quad (\text{A8})$$

Here, $|+\rangle = \frac{1}{|G|} \sum_{g \in G} |g\rangle$ is the equal-weighted superposition of all basis states.

The symmetries of this Hamiltonian are left and right group actions $\prod_v L_v^g$ and $\prod_v R_v^g$. However, throughout the rest of the paper, we will only focus on the right group action G^R and its gauging.

We can see that the Hamiltonian is a transverse-field Ising model because of its two limits. When $h_E = 0$, the ground state is given by a tensor product of $|+\rangle$ states and thus a paramagnet. When $h_E \rightarrow \infty$, the ground states are cat states, preferring to simultaneously point in the direction $|g\rangle$ for any $g \in G$, and therefore spontaneously breaks the global symmetry. We remark that for $G = \mathbb{Z}_N$, the Hamiltonian is simply the \mathbb{Z}_N Potts model.

We will now performing a Kramers-Wannier duality, which is also known as the ‘‘gauging map’’[8]. Heuristically, the map transforms ‘‘ G -spin’’ variables on vertices to ‘‘ G -domain-wall’’ variables on edges. The mapping from the vertex Hilbert space to the edge Hilbert space is that the state on each edge is determined from the two vertices it connects. Namely,

$$g_{i_e \rightarrow} \rightarrow g_{f_e} \rightarrow \xrightarrow{g_e} \quad (\text{A9})$$

where $g_e = g_{i_e} \bar{g}_{f_e}$. One can immediately notice that the map turns the Ising term Δ_e into a transverse field $|1\rangle \langle 1|_e$ for each edge, which is the projector T_e^1 .

Using this map, the operators and symmetries in the Hamiltonian map as

$$L_v^g \rightarrow \mathbf{A}_v^g = \prod_{e \rightarrow v} R_e^g \times \prod_{e \leftarrow v} L_e^g, \quad (\text{A10})$$

$$\Delta_e \rightarrow \sum_{g_e} \delta_{1, g_e} |g_e\rangle \langle g_e| = T_e^1, \quad (\text{A11})$$

$$\prod_v R_v^g \rightarrow \mathbb{1}. \quad (\text{A12})$$

Therefore, this procedure effectively ‘‘gauges’’ the right-multiplication symmetry G^R of the Hamiltonian.

Next, we notice that the map also produces constraints. For any plaquette p , we have the following identity

$$\prod_{e \in p} (g_{i_e} \bar{g}_{f_e})^{O(e)} = 1, \quad (\text{A13})$$

where the product is ordered clockwise around the plaquette. This implies that one must enforce the following fluxless condition

$$\prod_{e \in p} g_e^{O(e)} = 1 \quad (\text{A14})$$

in the gauged Hamiltonian, which we can enforce energetically with the term B_p . To conclude, the gauged Hamiltonian is

$$H_{\text{gauged}} = - \sum_v \mathbf{A}_v - h_E \sum_e T_e^1 - \sum_p \mathbf{B}_p, \quad (\text{A15})$$

which is precisely the model for $\mathcal{D}(G)$ under a transverse field introduced earlier. The gauging description here establishes that gauging a global symmetry of a G -paramagnet gives a G -topological order¹⁰.

2. Ising model and $\mathcal{D}(G)$ in the factored basis

Now, let us alternatively perform the gauging in two separate steps. First we will gauge a normal subgroup $N \triangleleft G$ to obtain a topological order with gauge group N enriched by the quotient group Q , and second, we then gauge Q . As a byproduct of two separate steps, we obtain an intermediate N -topological order with symmetry enrichment such as permutation and fractionalization of the anyons, which is encoded in the data of the group extension. We give examples for $G = D_4$ and different choices of normal subgroups N in Appendix C.

Using the factored system reviewed in section VA1, we can use it to “factor” a G d.o.f. into a N d.o.f. tensored with a Q d.o.f. That is, we can define a new basis $|n\rangle \otimes |q\rangle \in \mathbb{C}[N] \otimes \mathbb{C}[Q] \cong \mathbb{C}[G]$. We will refer to this basis as the *factored basis*. Let us write explicitly how the operators we defined previously are written in the factored basis. We start with left and right multiplications. To do this, we compute its action on a generic basis element $|g_e\rangle = |^{n_e}q_e\rangle$ in the factored basis.

$$L_e^g |g_e\rangle = |^n q \cdot ^{n_e} q_e\rangle = |\omega(q, q_e) n \sigma^q [n_e] q q_e\rangle \quad (\text{A16})$$

$$\begin{aligned} R_e^g |g_e\rangle &= |^{n_e} q_e \cdot \bar{n} \bar{q}\rangle = |^{n_e} q_e \cdot \bar{\omega}(\bar{q}, q) \sigma_{\bar{q}}[\bar{n}] \bar{q}\rangle \\ &= |\omega(q_e, \bar{q}) n_e \sigma^{q_e} [\bar{\omega}(\bar{q}, q) \sigma_{\bar{q}}[\bar{n}]] q_e \bar{q}\rangle \\ &= |^{n_e \bar{\omega}(q_e, \bar{q}) \sigma^{q_e \bar{q}}[\bar{n}]} q_e \bar{q}\rangle \end{aligned} \quad (\text{A17})$$

Therefore, using the controlled operators, the left and right multiplication in the factored basis acts as

$$L_e^g = (\mathbb{1} \otimes L_e^q) \times (L_e^{\Omega(q, e) n \Sigma_e^q} \otimes \mathbb{1}) \quad (\text{A18})$$

$$R_e^g = (R_e^{\Omega(e, q) \Sigma_e^q} \otimes \mathbb{1}) \times (\mathbb{1} \otimes R_e^q) \quad (\text{A19})$$

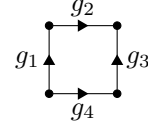
Note that the ordering of operators is of importance here.

Moving on to the Ising term in Eq. (A8), we can separate

it into two delta functions

$$\begin{aligned} \Delta_e &= \sum_{g_i, g_f} \delta_{1, g_i \bar{g}_f} |g_i, g_f\rangle \langle g_i, g_f| \\ &= \sum_{g_i, g_f} \delta_{1, t(g_i \bar{g}_f)} \delta_{1, \pi(g_i \bar{g}_f)} |g_i, g_f\rangle \langle g_i, g_f| \\ &= \sum_{n_i, n_f, q_i, q_f} \delta_{1, \bar{\omega}(q_i \bar{q}_f, q_f) n_i \sigma^{q_i \bar{q}_f} [\bar{n}_f]} \\ &\quad \delta_{1, q_i \bar{q}_f} |n_i, n_f, q_i, q_f\rangle \langle n_i, n_f, q_i, q_f| \end{aligned} \quad (\text{A20})$$

The terms in the quantum double Hamiltonian in Eq. (A3) can also be rewritten in the factored basis. The vertex term \mathbf{A}_v^g is the same using Eq. (A11) and the explicit form of left and right multiplications in the factored basis given above. For the plaquette term B_p , we can separate the expression into two delta functions, one of which contains only elements in Q . For simplicity, we derive the plaquette term for the square lattice. For a plaquette labeled as



The plaquette term is

$$B_p = \sum_{g_1, g_2, g_3, g_4} \delta_{1, g_1 g_2 \bar{g}_3 \bar{g}_4} |g_1, g_2, g_3, g_4\rangle \langle g_1, g_2, g_3, g_4| \quad (\text{A21})$$

Using the multiplication of the factor system, one finds

$$\begin{aligned} t(g_1 g_2 \bar{g}_3 \bar{g}_4) &= \omega(q_1, q_2) \omega(q_1 q_2, \bar{q}_3) \omega(q_1 q_2 \bar{q}_3, q_4) n_1 \\ &\quad \sigma^{q_1} [n_2] \sigma^{q_1 q_2} [\bar{\omega}(\bar{q}_3, q_3)] \sigma^{q_1 q_2 \bar{q}_3} [\bar{n}_3] \\ &\quad \sigma^{q_1 q_2 \bar{q}_3} [\bar{\omega}(\bar{q}_4, q_4)] \sigma^{q_1 q_2 \bar{q}_3 \bar{q}_4} [n_4] \end{aligned} \quad (\text{A22})$$

$$\pi(g_1 g_2 \bar{g}_3 \bar{g}_4) = q_1 q_2 \bar{q}_3 \bar{q}_4 \quad (\text{A23})$$

Thus, we obtain two delta functions setting the above two quantities to one. In addition, if we impose $q_1 q_2 \bar{q}_3 \bar{q}_4 = 1$ from the second delta function in addition to applying appropriate cocycle conditions, the first constraint simplifies to

$$\omega(q_1, q_2) \bar{\omega}(q_4, q_3) n_1 \sigma^{q_1} [n_2] \sigma^{q_4} [\bar{n}_3] n_4 = 1 \quad (\text{A24})$$

Therefore, the plaquette term in the factored basis is

$$\begin{aligned} B_p &= \sum_{\{n_i\}, \{q_i\}} \delta_{1, \omega(q_1, q_2) \bar{\omega}(q_4, q_3) n_1 \sigma^{q_1} [n_2] \sigma^{q_4} [\bar{n}_3] n_4} \\ &\quad \delta_{1, q_1 q_2 \bar{q}_3 \bar{q}_4} |\{n_i\}, \{q_i\}\rangle \langle \{n_i\}, \{q_i\}| \end{aligned} \quad (\text{A25})$$

3. Gauging N

As with gauging G , gauging a normal subgroup N can be thought of as a Kramers-Wannier duality which maps G -matter variables on vertices to a model with N -gauge variables on edges and Q -matter variables on vertices. The resulting model is a Symmetry-Enriched Topological (SET) order,

¹⁰ We note that after gauging there is still a residual global symmetry given by $G^L/Z(G) \cong \text{Inn}(G)$ in the quantum double model, but it is not relevant to our discussion.

an N -topological order enriched by a global symmetry Q . For each edge, the map is given by

$$g_i \rightarrow g_f \xrightarrow{n_e} q_i \rightarrow q_f \quad (\text{A26})$$

where

$$q_i = \pi(g_i), \quad q_f = \pi(g_f), \quad n_e = t(g_i \bar{g}_f). \quad (\text{A27})$$

Conceptually, the map can be thought of as a projection to Q variables via π and to N -domain walls via t . To work out how the operators in the Ising model map, we use the identities (35)-(39).

As an example, let us work out how L_v^g maps under the duality. Under the map, the operator L_v^g acts on the Q -d.o.f. at site v as L_v^q , but it also now act on the N -d.o.f. on edges surrounding v . For edges $e \rightarrow v$, L_v^g acts as left multiplication on i_e . Since such edge e has the d.o.f. $n_e = t(g_i \bar{g}_f)$, using Eq. (37), we obtain that the action of L_v^g on the dual d.o.f. sends n_e to $\bar{\omega}(q, q_i \bar{q}_f) n \sigma^q [n_e]$, which can be implemented via the gate $L_e^{\bar{\Omega}(q, v \bar{f}) n \Sigma_e^q}$. Similarly, for edges $e \leftarrow v$, we can use (38) to obtain the action of L_v^g on such edges. We conclude that under the duality,

$$L_v^g \rightarrow A_v^g = \prod_{e \rightarrow v} R_e^{\Omega(i \bar{v}, q) \Sigma^{i \bar{v}} [n]} \times L_v^q \times \prod_{e \leftarrow v} L_e^{\bar{\Omega}(q, v \bar{f}) n \Sigma_e^q}. \quad (\text{A28})$$

For the Ising term, it is apparent that

$$\Delta_e \rightarrow \tau_e = T_e^1 \sum_{q_i, q_f} \delta_{1, q_i \bar{q}_f} |q_i, q_f\rangle \langle q_i, q_f| \quad (\text{A29})$$

As for the symmetry, since $\prod_v R_v^g$ leaves $t(g_i \bar{g}_f)$ invariant for every edge, it only maps to right multiplication by q on every vertex.

$$\prod_v R_v^g \rightarrow \prod_v R_v^q \quad (\text{A30})$$

Finally, we enforce the constraints from this mapping energetically as a fluxless condition for each plaquette. We notice that by defining

$$\tilde{n}_e = \sigma^{\bar{q}_i} [\omega(q_i \bar{q}_f, q_f) n_e] = \sigma^{\bar{q}_i} [n_i] \sigma^{\bar{q}_f} [\bar{n}_f], \quad (\text{A31})$$

the product of the right hand side around a closed loop l (taking care of orientation) is the identity. Therefore,

$$\prod_{e \in l} \tilde{n}_e^{O_e} = 1. \quad (\text{A32})$$

This constraint can be enforced energetically via the following plaquette term

$$B_p^N = \sum_{\{n_e, q_v\}} \delta_{1, \prod_{e \subset p} \tilde{n}_e^{O_e} \{n_e, q_v\}} \langle \{n_e, q_v\} \rangle. \quad (\text{A33})$$

To conclude, the Hamiltonian for the SET is

$$H_{SET} = -\frac{1}{|G|} \sum_v \left(\sum_{g \in G} A_v^g \right) - h_E \sum_e \tau_e - \sum_p B_p^N \quad (\text{A34})$$

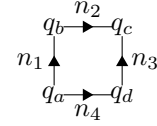
4. Gauging Q of the SET

We would now like to gauge the remaining Q symmetry of the SET using the gauging map $|q_i, q_f\rangle \rightarrow |q_i \bar{q}_f\rangle$. For the vertex term A_v^g , first, we can replace $i \bar{v}$ and $v \bar{f}$ with e for edges $e \rightarrow v$ and $e \leftarrow v$ in Eq. (A28), respectively. In addition, we gauge the second term L_v^q to $\prod_{e \rightarrow v} R_e^q \times \prod_{e \leftarrow v} L_e^q$ as usual. Keeping track of the tensor products, we obtain

$$A_v^g \rightarrow \mathbf{A}_v^g = \prod_{e \rightarrow v} \left(R_e^{\Omega(e, q) \Sigma^e [n]} \otimes \mathbb{1} \right) \times \prod_{e \rightarrow v} (\mathbb{1} \otimes R_e^q) \\ \times \prod_{e \leftarrow v} (\mathbb{1} \otimes L_e^q) \times \prod_{e \leftarrow v} \left(L_e^{\bar{\Omega}(q, e) n \Sigma_e^q} \otimes \mathbb{1} \right). \quad (\text{A35})$$

Finally, using Eqs.(A18)-(A19), we see that the expression matches \mathbf{A}_v^g in the unfactored basis (A11) as expected.

To gauge the plaquette term, B_p^N , we will do this on the square lattice for simplicity. We label the vertices and edges with variables as shown



Then, the constraint of the delta function of B_p^N in Eq. (A33) reads

$$\sigma^{\bar{q}_{i_1}} [\omega(q_{i_1} \bar{q}_{f_1}, q_{f_1}) n_1] \sigma^{\bar{q}_{i_2}} [\omega(q_{i_2} \bar{q}_{f_2}, q_{f_2}) n_2] \\ \sigma^{\bar{q}_{i_3}} [\bar{\omega}(q_{i_2} \bar{q}_{f_3}, q_{f_3}) \bar{n}_3] \sigma^{\bar{q}_{i_4}} [\bar{\omega}(q_{i_4} \bar{q}_{f_4}, q_{f_4}) n_4] = 1 \quad (\text{A36})$$

From the figure, we can relabel the sites $i_1 = i_4 \equiv a$, $f_1 = i_2 \equiv b$, $f_2 = f_3 \equiv c$, $f_4 = i_3 \equiv d$. We apply σ_{q_a} on both sides to obtain

$$\omega(q_a \bar{q}_b, q_b) \sigma^{q_a \bar{q}_b} [\omega(q_b \bar{q}_c, q_c)] \sigma^{q_a \bar{q}_d} [\bar{\omega}(q_d \bar{q}_c, q_c)] \\ \bar{\omega}(q_a \bar{q}_d, q_d) n_1 \sigma^{q_a \bar{q}_b} [n_2] \sigma^{q_a \bar{q}_d} [\bar{n}_3] n_4 = 1 \quad (\text{A37})$$

Using the cocycle conditions to get rid of the cocycles with σ acting on them, the expression simplifies to

$$\omega(q_a \bar{q}_b, q_b \bar{q}_c) \bar{\omega}(q_a \bar{q}_d, q_d \bar{q}_c) n_1 \sigma^{q_a \bar{q}_b} [n_2] \sigma^{q_a \bar{q}_d} [\bar{n}_3] n_4 = 1 \quad (\text{A38})$$

We can now use the gauging map

$$q_a \bar{q}_b \rightarrow q_1 \quad q_b \bar{q}_c \rightarrow q_2 \quad q_d \bar{q}_c \rightarrow q_3 \quad q_a \bar{q}_d \rightarrow q_4 \quad (\text{A39})$$

to map the above constraint to

$$\omega(q_1, q_2) \bar{\omega}(q_4, q_3) n_1 \sigma^{q_1} [n_2] \sigma^{q_4} [\bar{n}_3] n_4 = 1 \quad (\text{A40})$$

which is exactly the constraint that appears in Eq. (A24). The plaquette term of the SET therefore gauges to

$$B_p^N \rightarrow \mathbf{B}_p^N = \sum_{\{n_e, q_e\}} \delta_{1, \omega(q_1, q_2) \bar{\omega}(q_4, q_3) n_1 \sigma^{q_1} [n_2] \sigma^{q_4} [\bar{n}_3] n_4} \\ \langle \{n_e, q_e\} \rangle \langle \{n_e, q_e\} \rangle \quad (\text{A41})$$

TABLE VI. Mapping of operators in the G -Ising model, the SET (N -topological order enriched by Q), and the quantum double $\mathcal{D}(G)$ in the factored basis. Here, the operators are defined on a square lattice for simplicity.

G -Ising	SET	$\mathcal{D}(G)$
L_v^g	$A_v^g = \prod_{e \rightarrow v} R_e^{\Omega(i\bar{v}, q)\Sigma^{\bar{v}}[n]} \times L_v^g \times \prod_{e \leftarrow v} L_e^{\Omega(q, v\bar{f})n\Sigma^q}$	$A_v^g = \prod_{e \rightarrow v} \left[(R_e^{\Omega(e, q)\Sigma^e[n]} \otimes \mathbb{1}) \times (\mathbb{1} \otimes R_e^g) \right] \times \prod_{e \leftarrow v} \left[(\mathbb{1} \otimes L_e^g) \times (L_e^{\Omega(q, e)n\Sigma_e^g} \otimes \mathbb{1}) \right]$
Δ_e	$\tau_e = T_e^1 \sum_{q_i, q_f} \delta_{1, q_i \bar{q}_f} q_i, q_f\rangle \langle q_i, q_f $	$\tau_e = T_e^1 \otimes T_e^1$
1	$B_p^N = \sum_{\{n_e, q_v\}} \delta_{1, \prod_{e \subset p} \bar{n}_e} O_e \{n_e, q_v\}\rangle \langle \{n_e, q_v\} $	$B_p^N = \sum_{\{n_e, q_e\}} \delta_{1, \omega(q_1, q_2)\bar{\omega}(q_4, q_3)n_1\sigma^{q_1}[n_2]\sigma^{q_4}[\bar{n}_3]n_4} \{n_e, q_e\}\rangle \langle \{n_e, q_e\} $
1	1	$B_p^Q = \sum_{\{q_e\}} \delta_{1, q_1 q_2 \bar{q}_3 \bar{q}_4} \{q_e\}\rangle \langle \{q_e\} $
$\prod_v R_v^g$	$\prod_v R_v^g$	1

In addition, we also need to enforce a fluxless condition for the new Q variables on each plaquette. This is done via

$$B_p^Q = \sum_{\{q_e\}} \delta_{1, q_1 q_2 \bar{q}_3 \bar{q}_4} |\{q_e\}\rangle \langle \{q_e\}| \quad (\text{A42})$$

Therefore, after gauging Q of the SET, we obtain

$$H_{\text{gauged SET}} = - \sum_v \mathbf{A}_v - h_E \sum_e (T_e^1 \otimes T_e^1) - \sum_p \left(B_p^N + B_p^Q \right) \quad (\text{A43})$$

It is important to note that the Hamiltonian above is not exactly the quantum double Hamiltonian (under a transverse field) defined in Eq. (A3). To be precise, although the \mathbf{A}_v terms match exactly, the plaquette terms B_p differ. The reason is because by performing two separate gaugings, we have imposed fluxless conditions on two occasions, which resulted in two separated plaquette terms B_p^N and B_p^Q rather than a single plaquette term B_p of the quantum double model. Nevertheless, since the two plaquette terms are commuting projectors and $B_p^N B_p^Q = B_p$, the two Hamiltonians have the same ground state, and therefore describe the same topological order.

To summarize the dualities, we list the result of operators under the gauging map, first by gauging N followed by gauging Q in Table VI.

Appendix B: Gauging G via minimal coupling

In this appendix, we use the minimal coupling procedure instead of the Kramers-Wannier duality to demonstrate the mapping from a G -Ising model to a G -topological order under a transverse field.[5, 7]

The minimal coupling procedure we will perform promotes the right multiplication symmetry G^R into a local symmetry. We add G gauge fields living on each edge and impose the

following Gauss law on each vertex

$$\mathcal{G}_v = \frac{1}{|G|} \sum_g \mathcal{G}_v^g = 1 \quad (\text{B1})$$

$$\mathcal{G}_v^g = \left(\prod_{e \rightarrow v} R_e^g \right) R_v^g \left(\prod_{e \leftarrow v} L_e^g \right) \quad (\text{B2})$$

It is apparent that \mathcal{G}_v^g on different vertices commute. Therefore, the Gauss law on different vertices commute. Furthermore, \mathcal{G}_v^g obeys the group law of G , and they therefore implement a local symmetry transformation. Multiplying \mathcal{G}_v^g on all vertices, we obtain

$$\prod_v R_v^g \prod_e (L_e^g R_e^g), \quad (\text{B3})$$

which, after further removing the conjugation symmetry on the edge (gauge) variables, recovers the global G^R symmetry.

Next, we must minimally couple the Hamiltonian so that it commutes with the Gauss law. The minimally coupled term is

$$\Delta_e^{\text{MC}} = \sum_{g_i, g_e, g_f} \delta_{1, g_i g_e g_f^{-1}} |g_i, g_e, g_f\rangle \langle g_i, g_e, g_f|. \quad (\text{B4})$$

One can see that it commutes with each \mathcal{G}_v^g , and therefore commutes with \mathcal{G}_v . The projector $|+\rangle \langle +|$ already commutes with the Gauss law and so it does not need to be modified. Finally we enforce a ‘‘fluxless’’ condition around each plaquette p . Similarly, we enforce this energetically using B_p defined in the main text. The minimally coupled Hamiltonian reads

$$H^{\text{MC}} = - \sum_e \Delta_e^{\text{MC}} - h \sum_v L_v - \Lambda \sum_p B_p; \quad \mathcal{G}_v = 1 \quad (\text{B5})$$

Next, we will compute the effective Hamiltonian obtained by restricting the Hilbert space using the Gauss law, and show that it is the quantum double model under a transverse field. To do so, we will perform a change of basis using a unitary U such that the Gauss law becomes

$$U \mathcal{G}_v U^\dagger = \frac{1}{|G|} \sum_{g \in G} R_v^g = 1 \quad (\text{B6})$$

The unitary is given by

$$U = \prod_v \left[\prod_{e \rightarrow v} CR_{ve} \prod_{e \leftarrow v} CL_{ve} \right] \quad (\text{B7})$$

where

$$CL_{ve} : |a\rangle_v |b\rangle_e \rightarrow |a\rangle_v |ab\rangle_e \quad (\text{B8})$$

$$CR_{ve} : |a\rangle_v |b\rangle_e \rightarrow |a\rangle_v |b\bar{a}\rangle_e \quad (\text{B9})$$

are controlled left and right multiplication operators[62], which satisfy the following identities

$$CL_{ve}(L_v^g \otimes \mathbb{1}_e)CL_{ve}^{-1} = L_v^g \otimes L_e^g, \quad (\text{B10})$$

$$CR_{ve}(L_v^g \otimes \mathbb{1}_e)CL_{ve}^{-1} = L_v^g \otimes R_e^g, \quad (\text{B11})$$

$$CL_{ve}(R_v^g \otimes L_e^g)CL_{ve}^{-1} = R_v^g \otimes \mathbb{1}_e, \quad (\text{B12})$$

$$CR_{ve}(R_v^g \otimes R_e^g)CR_{ve}^{-1} = R_v^g \otimes \mathbb{1}_e. \quad (\text{B13})$$

The minimally coupled kinetic term in the new basis is

$$\begin{aligned} U\Delta^{\text{MC}}U^\dagger &= \sum_{g_i, g_e, g_f} U\Delta^{\text{MC}} |g_i, \bar{g}_i g_e g_f, g_f\rangle \langle g_i, g_e, g_f| \\ &= \sum_{g_i, g_e, g_f} U\delta_{1, g_i(\bar{g}_i g_e g_f)\bar{g}_f} |g_i, \bar{g}_i g_e g_f, g_f\rangle \langle g_i, g_e, g_f| \\ &= \sum_{g_i, g_e, g_f} \delta_{1, g_e} |g_i, g_e, g_f\rangle \langle g_i, g_e, g_f| = |1\rangle \langle 1|_e \end{aligned} \quad (\text{B14})$$

A similar calculation shows that B_p is invariant under U . Therefore,

$$\begin{aligned} UH^{\text{MC}}U^\dagger &= - \sum_v \left[\frac{1}{|G|} \sum_{g \in G} \left(\prod_{e \rightarrow v} R_e^g \right) L_v^g \left(\prod_{e \leftarrow v} L_e^g \right) \right] \\ &\quad - h_{\text{Ising}} \sum_e |1\rangle \langle 1|_e - \sum_p B_p \end{aligned} \quad (\text{B15})$$

with Gauss law $U\mathcal{G}_vU^\dagger = \frac{1}{|G|} \sum R_v^g = 1$

Now, we restrict to the subspace invariant under the Gauss law, which is the singlet $|+\rangle_v$ for every vertex. This means that L_v^g acts as the trivial irrep in this subspace so we can replace $L_v^g = 1$ for all g . The result is the effective Hamiltonian

$$\begin{aligned} H_{\text{gauge}} &= - \sum_v \left[\frac{1}{|G|} \sum_{g \in G} \left(\prod_{e \rightarrow v} R_e^g \right) \left(\prod_{e \leftarrow v} L_e^g \right) \right] \\ &\quad - h_{\text{Ising}} \sum_e |1\rangle \langle 1|_e - \sum_p B_p \end{aligned} \quad (\text{B16})$$

This is the quantum double model under a transverse field.

Appendix C: Examples of Symmetry Enrichment in Topological and Fracton Phases

In this Appendix, we give examples of symmetry fractionalization in topological and fracton phases. We emphasize that the phenomena of the former has already been established both mathematically[44] and explicitly via lattice

models[45, 46]. Various other constructions including those that perform a general permutation and fractionalization have also been demonstrated [63–68]. Nevertheless, we find it insightful to demonstrate the enrichment properties explicitly for the SETs we present in Appendix A 3 since it generalizes naturally to the fracton case where a global symmetry permutes or fractionalizes the fractonic excitations as presented in the main text.

1. Permutation and Fractionalization in the SET

Starting with the SET Hamiltonian (A34), we will perform a basis transformation to turn the N -d.o.f. on edges from n_e to \tilde{n}_e defined in Eq. (A31). In this basis, the d.o.f. on N forms the quantum double model $D(N)$, which can be partially seen from the expression of the plaquette term B_p^N (A33). We can then explicitly demonstrate the enrichment via the symmetry Q via the fractionalization and permutation of anyons.

There are two ways in which this basis transformation can be achieved. The first is to conjugate the Hamiltonian by the following change of basis unitary

$$U = \prod_e \sum_i L_e^{\Omega(i\bar{f}, f)}. \quad (\text{C1})$$

The second is to use the following gauging map instead of Eq. (A26) to dualize the G -Ising model.

$$g_i \rightarrow g_f \rightarrow q_i \xrightarrow{\tilde{n}_e} q_f \quad (\text{C2})$$

with \tilde{n}_e defined as Eq. (A31).

The two methods are equivalent. Here we will choose to present the second method to calculate the form of the operators, which we will note with tildes to contrast them from the operators in the basis of Eq. (A34) presented earlier. That is, all terms with tildes are related to the ones without tildes via a conjugation of U .

First, we will need to derive how the expression $\sigma^{qv} [n_v]$ transforms under left and right multiplication. They are

$$L^g : \sigma^{qv} [n_v] \rightarrow \sigma^{\bar{q}q} [\omega(q, q_v)n\sigma^q [n_v]] \quad (\text{C3})$$

$$L^g : \sigma^{qv} [\tilde{n}_v] \rightarrow \sigma^{\bar{q}q} [\overline{\omega(q, q_v)n\sigma^q [n_v]}] \quad (\text{C4})$$

$$R^{\bar{g}} : \sigma^{qv} [n_v] \rightarrow \sigma^{q\bar{q}} [\omega(q_v, q)n_v\sigma^{qv} [n]] \quad (\text{C5})$$

$$R^{\bar{g}} : \sigma^{qv} [\tilde{n}_v] \rightarrow \sigma^{q\bar{q}} [\overline{\omega(q_v, q)n_v\sigma^{qv} [n]}] \quad (\text{C6})$$

Using this, we can figure out how the global symmetry $\prod_v R_v^{\bar{g}}$ maps. In addition to acting as $R_v^{\bar{g}}$ on all vertices, it also has a non-trivial action on \tilde{n}_e

$$\begin{aligned} \prod_v R_v^{\bar{g}} : \tilde{n}_e &= \sigma^{\bar{q}_i} [n_i] \sigma^{\bar{q}_f} [\tilde{n}_f] \\ &\rightarrow \sigma^{q\bar{q}_i} [\omega(q_i, q)n_i\sigma^{q_i} [n]] \sigma^{q\bar{q}_f} [\overline{\omega(q_f, q)n_f\sigma^{q_f} [n]}] \\ &= \sigma^q [\sigma^{\bar{q}_i} [\omega(q_i, q)] \sigma^{\bar{q}_f} [\overline{\omega(q_f, q)}] \tilde{n}_e] \end{aligned} \quad (\text{C7})$$

Therefore, the global G^R symmetry dualizes to

$$\prod_v R_v^g \rightarrow \prod_v R_v^q \times \prod_e \Sigma_e^q \times \prod_e L_e^{\Sigma_e^{\bar{i}[\Omega_e(i,q)]\Sigma_e^{\bar{f}[\Omega_e(f,q)]}} \quad (\text{C8})$$

So in this basis, the remaining Q^R symmetry is no longer on-site when ω is a non-trivial cocycle.

Next, let us map L_v^g . For edges $e \rightarrow v$, $v = i_e$, so \tilde{n}_e transforms as

$$\begin{aligned} L_v^g : \tilde{n}_e &\rightarrow \sigma^{\bar{q}v} [\omega(q, q_v) n \sigma^q [n_v]] \sigma^{\bar{q}f} [\tilde{n}_f] \\ &= \sigma^{\bar{q}v} [\omega(q, q_v) n] \tilde{n}_e \end{aligned} \quad (\text{C9})$$

And for edges $e \leftarrow v$, $v = f_e$, so \tilde{n}_e transforms as

$$\begin{aligned} L_v^g : \tilde{n}_e &\rightarrow \sigma^{\bar{q}i} [n_i] \sigma^{\bar{q}v\bar{q}} [\omega(q, q_v) n \sigma^q [n_v]] \\ &= \sigma^{\bar{q}v} [\bar{\omega}(q, q_v) \bar{n}] \tilde{n}_e \end{aligned} \quad (\text{C10})$$

Therefore, we see that the action on the dual variables is

$$L_v^g \rightarrow \tilde{A}_v^g = \prod_{e \rightarrow v} R_e^{\Sigma_e^{\bar{v}[\Omega(q, \bar{q}q_v) n]}} \times \prod_{e \leftarrow v} L_e^{\Sigma_e^{\bar{v}[\Omega(q, \bar{q}q_v) n]}} \times L_v^q \quad (\text{C11})$$

In particular, we see that for elements n^1 in the embedded normal subgroup

$$\tilde{A}_v^{n^1} = \prod_{e \rightarrow v} R_e^{\Sigma_e^{\bar{v}[n]}} \times \prod_{e \leftarrow v} L_e^{\Sigma_e^{\bar{v}[n]}}. \quad (\text{C12})$$

This is precisely the vertex term of $\mathcal{D}(N)$ up to an action by σ , which we will later demonstrate is responsible for permutation of anyons.

The constraints from the mapping is still given by Eq. (A32). However, since we are already in the \tilde{n}_e basis, the form of the operator we enforce is

$$\tilde{B}_p^N = \sum_{\{\tilde{n}_e\}} \delta_{1, \prod_{e \subset p} \tilde{n}_e^{O_e}} |\{\tilde{n}_e\}\rangle \langle \{\tilde{n}_e\}|. \quad (\text{C13})$$

This is just the plaquette term of $\mathcal{D}(N)$. To conclude, we have performed a basis transformation into a basis where the N -d.o.f. form the quantum double model $\mathcal{D}(N)$

a. Examples: $G = D_4$

To give explicit examples of symmetry fractionalization and permutation, we will analyze three examples of $G = D_4 = \langle r, s | r^4 = s^2 = (sr)^2 = 1 \rangle$ with different choices of N . A stack of the examples here are in fact the realizations of the symmetry enrichment of the 1-foliated examples discussed in Sec. III A after gauging N .

1. $N = \mathbb{Z}_2 = \langle r^2 | (r^2)^2 = 1 \rangle$ and $Q = \mathbb{Z}_2^2 = \langle r, s | r^2 = s^2 = (rs)^2 = 1 \rangle$ are representative elements of each coset. The extension is a central extension with cocycle specified by

$$\omega(r, r) = r^2, \quad \omega(s, s) = \omega(rs, rs) = 1. \quad (\text{C14})$$

Note that the action of the cocycle on the other group elements are fixed by consistency using the cocycle condition. The vertex operators of interest are

$$\tilde{A}_v^{r^2} = - \begin{array}{c} X \diagup \\ X \diagdown \\ X \end{array} \quad (\text{C15})$$

$$\tilde{A}_v^{rs} = (XI)_v \left(- \begin{array}{c} X \diagup \\ X \diagdown \\ X \end{array} \right)^{\frac{1-(IZ)_v}{2}} \quad (\text{C16})$$

$$\tilde{A}_v^s = (IX)_v \quad (\text{C17})$$

$$\tilde{A}_v^r = (XX)_v \left(- \begin{array}{c} X \diagup \\ X \diagdown \\ X \end{array} \right)^{\frac{1+(IZ)_v}{2}} \quad (\text{C18})$$

where we have suppressed tensor products for simplicity. The above vertex operators generate all other \tilde{A}_v^g operators. As for the plaquette term, we have

$$\tilde{B}_p^N = \frac{1 + \tilde{B}_p^{r^2}}{2} \quad (\text{C19})$$

where

$$\tilde{B}_p^{r^2} = \begin{array}{c} \diagdown \quad \diagup \\ \diagup \quad \diagdown \end{array} \quad (\text{C20})$$

The global \mathbb{Z}_2^2 symmetry is generated by $\prod_v \tilde{S}_v^{rs}$ and $\prod_v \tilde{S}_v^s$ where

$$\tilde{S}_v^{rs} = (XI)_v \quad (\text{C21})$$

$$\tilde{S}_v^s = (IX)_v \times (\tilde{A}_v^{r^2})^{\frac{1-(ZI)_v}{2}} \quad (\text{C22})$$

This global symmetry squares to one and commutes with the terms above. Now, let us now compute the local symmetry action on a single vertex v . We find $(\tilde{S}_v^{rs})^2 = (\tilde{S}_v^s)^2 = 1$, but

$$(\tilde{S}_v^r)^2 = (\tilde{S}_v^{rs} \tilde{S}_v^s)^2 = \tilde{A}_v^{r^2} \quad (\text{C23})$$

Therefore, for an excited state where an anyon e is positioned at vertex v , we have $\tilde{A}_v^{r^2} = -1$, which gives the desired fractionalization

$$(\tilde{S}_v^r)^2 = -1. \quad (\text{C24})$$

2. $N = \mathbb{Z}_2^2 = \langle r^2, rs | (r^2)^2 = (rs)^2 = (r^3s)^2 = 1 \rangle$ and $Q = \mathbb{Z}_2 = \langle r | r^2 = 1 \rangle$. The extension is instead a split extension ($G = N \rtimes Q$), so $\omega(q, q') = 1$. σ_r acts as

$$\sigma_r[rs] = \bar{r}s \quad \sigma_{rs}[\bar{r}s] = rs \quad \sigma_r[r^2] = r^2 \quad (\text{C25})$$

Therefore, it is convenient to choose the Pauli operators to be in the basis generated by rs and $\bar{r}s$, so that the global \mathbb{Z}_2 acts as a swap on the two copies of the toric code. In this basis, the operators are

$$\tilde{A}_v^{rs} = \left(\begin{array}{c} \diagup \\ -XI \\ \diagdown \\ \diagdown \\ XI \\ \diagup \end{array} \right)^{\frac{1+Z_v}{2}} \left(\begin{array}{c} \diagup \\ -IX \\ \diagdown \\ \diagdown \\ IX \\ \diagup \end{array} \right)^{\frac{1-Z_v}{2}} \quad (\text{C26})$$

$$\tilde{A}_v^{\bar{r}s} = \left(\begin{array}{c} \diagup \\ -XI \\ \diagdown \\ \diagdown \\ XI \\ \diagup \end{array} \right)^{\frac{1-Z_v}{2}} \left(\begin{array}{c} \diagup \\ -IX \\ \diagdown \\ \diagdown \\ IX \\ \diagup \end{array} \right)^{\frac{1+Z_v}{2}} \quad (\text{C27})$$

$$\tilde{A}_v^r = X_v \quad (\text{C28})$$

The flux term can be decomposed as

$$\tilde{B}_p^N = \frac{1 + \tilde{B}_p^{rs}}{2} \cdot \frac{1 + \tilde{B}_p^{\bar{r}s}}{2} \quad (\text{C29})$$

where

$$\tilde{B}_p^{rs} = \begin{array}{c} \diagup \\ ZI \\ \diagdown \\ \diagdown \\ ZI \\ \diagup \end{array} \quad (\text{C30})$$

$$\tilde{B}_p^{\bar{r}s} = \begin{array}{c} \diagup \\ IZ \\ \diagdown \\ \diagdown \\ IZ \\ \diagup \end{array} \quad (\text{C31})$$

and the \mathbb{Z}_2 symmetry acts as $\prod_v X_v \cdot \prod_e \text{SWAP}_e$ where

$$\text{SWAP} = \begin{pmatrix} 1 & 0 & 0 & 0 \\ 0 & 0 & 1 & 0 \\ 0 & 1 & 0 & 0 \\ 0 & 0 & 0 & 1 \end{pmatrix}. \quad (\text{C32})$$

A pair of pure charge and pure fluxes in the bilayer toric code labeled e_1, e_2, m_1 and m_2 are created using strings of XI, IX, ZI , and IZ respectively. Therefore, we see that under the \mathbb{Z}_2 symmetry the string operators are swapped, permuting the anyons at the ends of the string.

3. $N = \mathbb{Z}_4 = \langle r | r^4 = 1 \rangle$ and $Q = \mathbb{Z}_2 = \langle s | s^2 = 1 \rangle$. The extension is also a split extension, so $\omega(q, q') = 1$ and σ_s acts as charge conjugation \mathcal{C} on the N variables. We will use Pauli matrices Z, X on Q variables, \mathbb{Z}_4 clock and shift matrices \mathcal{Z}, \mathcal{X} on N variables, and use bars for the Hermitian conjugate (e.g. $\mathcal{C}\mathcal{X}\mathcal{C} = \bar{\mathcal{X}}$). The operators are

$$\tilde{A}_v^r = \left(\begin{array}{c} \diagup \\ -\bar{\mathcal{X}} \\ \diagdown \\ \diagdown \\ \bar{\mathcal{X}} \\ \diagup \end{array} \right)^{Z_v} \quad (\text{C33})$$

$$\tilde{A}_v^s = X_v \quad (\text{C34})$$

The flux term can be written as

$$B_p^N = \frac{1 + B_p^r + (B_p^r)^2 + (B_p^r)^3}{4} \quad (\text{C35})$$

where

$$\tilde{B}_p^r = \begin{array}{c} \diagup \\ \bar{\mathcal{Z}} \\ \diagdown \\ \diagdown \\ \bar{\mathcal{Z}} \\ \diagup \end{array} \quad (\text{C36})$$

and the \mathbb{Z}_2 symmetry acts as $\prod_v X_v \prod_e \mathcal{C}_e$, where

$$\mathcal{C} = \begin{pmatrix} 1 & 0 & 0 & 0 \\ 0 & 0 & 0 & 1 \\ 0 & 0 & 1 & 0 \\ 0 & 1 & 0 & 0 \end{pmatrix} \quad (\text{C37})$$

is the charge conjugation operator. Thus, we have written the model in the basis of the \mathbb{Z}_4 toric code, with gauge charges generated by e and gauge fluxes generated by m . Here, an $e - \bar{e}$ pair is created by a string of \mathcal{Z} , and an $m - \bar{m}$ pair is excited with a string of \mathcal{X} operators on the dual lattice. The strings are charge conjugated under the global \mathbb{Z}_2 symmetry, which means the the symmetry permutes both e and m the anyons according to charge conjugation.

2. Permutation and Fractionalization in the SEF

Identically to the previous section, we will perform a basis transformation on the SEF Hamiltonian (87) on the N -d.o.f. of each plaquette from n_p to \tilde{n}_p defined in Eq. (82) reproduced here

$$\begin{aligned} \tilde{n}_p &= \sigma^{\bar{q}_i} [\omega(q_i \bar{q}_j, q_j) \bar{\omega}(q_i \bar{q}_k, q_k) \omega(q_i \bar{q}_l, q_l) n_p] \\ &= \sigma^{\bar{q}_i} [n_i] \sigma^{\bar{q}_j} [\bar{n}_j] \sigma^{\bar{q}_k} [n_k] \sigma^{\bar{q}_l} [\bar{n}_l], \end{aligned} \quad (\text{C38})$$

One way to do this is to conjugate the Hamiltonian by the following change of basis unitary

$$U = \prod_p \sum_i L_p^{\Omega_e(i\bar{j}, j) \bar{\Omega}_e(i\bar{k}, k) \Omega_e(i\bar{l}, l)} \quad (\text{C39})$$

The second is to use the following gauging map instead of Eq.(73) to dualize the (G, N) -Ising model.

$$\begin{array}{ccc} g_l & \text{---} & g_k \\ | & & | \\ g_i & \text{---} & g_j \end{array} \rightarrow \begin{array}{ccc} q_l & \text{---} & q_k \\ | & & | \\ q_i & \text{---} & q_j \end{array} \quad \begin{array}{c} \tilde{n}_p \\ \hline \end{array} \quad (\text{C40})$$

In an identical calculation to Appendix C1, we can calculate how the operators and symmetries act under this map using Eqs. (C3)-(C6). The results are

$$\prod_v R_v^{\bar{g}} \rightarrow \prod_v R_v^{\bar{q}} \times \prod_p \Sigma_p^{\bar{q}} \quad (\text{C41})$$

$$\begin{aligned} &\times \prod_p L_p^{\Sigma^i[\Omega(i, q)] \Sigma^j[\bar{\Omega}(j, q)] \Sigma_p^k[\Omega(k, q)] \Sigma^f[\bar{\Omega}(l, q)]} \\ L_v^g &\rightarrow \tilde{A}_v^g = \prod_{p|v=j, l} R_p^{\Sigma^{\bar{q}}[\Omega(q, \bar{q}q_v) n]} \\ &\times \prod_{p|v=i, k} L_p^{\Sigma^{\bar{q}}[\Omega(q, \bar{q}q_v) n]} \times L_v^q \end{aligned} \quad (\text{C42})$$

with constraints

$$\tilde{B}_{c,x}^N = \sum_{\{\tilde{n}\}} \delta_{1, \tilde{n}_y \bar{\tilde{n}}_z \bar{\tilde{n}}_{\bar{y}} \tilde{n}_{\bar{z}}} |\{\tilde{n}\}\rangle \langle \{\tilde{n}\}| \quad (\text{C43})$$

TABLE VII. Examples of possible hybrid fracton models constructed from different choices of groups N and Q . Here, the subsystem symmetry is chosen to be three intersecting planes (3-foliated). A hybrid model (blue) is obtained for any G that is a non-trivial group extension of Q by N . References are included for models that have appeared in previous works. The (G, N) gauge theories give a unified perspective of these models.

N	Q	G	Description
\mathbb{Z}_1	\mathbb{Z}_1	\mathbb{Z}_1	Trivial
\mathbb{Z}_1	\mathbb{Z}_2	\mathbb{Z}_2	\mathbb{Z}_2 TC
\mathbb{Z}_2	\mathbb{Z}_1	\mathbb{Z}_2	\mathbb{Z}_2 X-cube
\mathbb{Z}_2	\mathbb{Z}_2	\mathbb{Z}_2^2 \mathbb{Z}_4	\mathbb{Z}_2 TC \otimes \mathbb{Z}_2 X-cube Fractonic Hybrid X-cube[1]
\mathbb{Z}_2	\mathbb{Z}_2^2	\mathbb{Z}_2^3 $\mathbb{Z}_4 \times \mathbb{Z}_2$ D_4 Q_8	\mathbb{Z}_2^2 X-cube \otimes \mathbb{Z}_2 TC Fractonic Hybrid X-cube \otimes \mathbb{Z}_2 TC D_4 hybrid model (all abelian charges mobile)[22] Q_8 hybrid model (all abelian charges mobile)
\mathbb{Z}_2^2	\mathbb{Z}_2	\mathbb{Z}_2^3 $\mathbb{Z}_4 \times \mathbb{Z}_2$ D_4	\mathbb{Z}_2^2 X-cube \otimes \mathbb{Z}_2 TC Fractonic Hybrid X-cube \otimes \mathbb{Z}_2 X-cube D_4 hybrid model (r mobile)[27–29, 36]
\mathbb{Z}_3	\mathbb{Z}_2	$\mathbb{Z}_3 \times \mathbb{Z}_2$ S_3	\mathbb{Z}_3 X-cube \otimes \mathbb{Z}_2 TC S_3 hybrid model[36]
\mathbb{Z}_4	\mathbb{Z}_2	$\mathbb{Z}_4 \times \mathbb{Z}_2$ \mathbb{Z}_8 D_4 Q_8	\mathbb{Z}_4 X-cube \otimes \mathbb{Z}_2 TC \mathbb{Z}_8 hybrid model (one mobile charge) D_4 hybrid model (s mobile) Q_8 hybrid model (one mobile abelian charge)

This, along with its C_3 rotations are the cube terms of the X-cube model with gauge group N . Furthermore, for $g = {}^n 1$, we see that

$$\tilde{A}_v^{n1} = \prod_{p|v=j,l} R_p^{\Sigma^v[n]} \prod_{p|v=i,k} L_p^{\Sigma^v[n]} \quad (\text{C44})$$

is the vertex term of the X-cube model up to a possible action by σ . The symmetry permutation and fractionalization of the fractons/lineons can be analogously shown for the three choices of normal subgroups in D_4 by replacing the the \tilde{A}_v and \tilde{B}_p of the toric code in 2D with \tilde{A}_v and $\tilde{B}_{c,r}$ of the X-cube model in 3D.

Appendix D: Examples of 3-foliated hybrid models

In this Appendix, we give examples of 3-foliated hybrid models by specifying the groups in our commuting projector Hamiltonian (24). In Table VII, we enumerate the hybrid fracton models that can be constructed given abelian groups N and Q , many of which hosts non-abelian fractons.

1. $(\mathbb{Z}_4, \mathbb{Z}_2)$

As a sanity check, we show that the resulting model for $(\mathbb{Z}_4, \mathbb{Z}_2)$ has the same ground state as the fractonic hybrid X-cube model presented in Ref. 1.

We represent $N = \langle r | r^2 = 1 \rangle$ and $Q = \langle s | s^2 = 1 \rangle$. The group extension is a central extension whose factor system is given by $\sigma = 1$ and non-trivial cocycle $\omega(s, s) = r$.

Starting with \mathbf{A}_v^g , the expressions reduce to the Pauli matri-

ces as follows

$$R_p^r = L_p^r \equiv X_p \quad (\text{D1})$$

$$R_e^s = L_e^s \equiv X_e \quad (\text{D2})$$

$$L_p^{\Omega(e,s)} = R_p^{\Omega(e,s)} \equiv X_p^{\frac{1-Z_e}{2}} \quad (\text{D3})$$

With this, we find

$$\begin{aligned} \mathbf{A}_v^{1s} &= \prod_{p|v=j,k,l} X_p^{\frac{1-Z_{iv}}{2}} \times \prod_{e \supset v} X_e \\ &\times \prod_{p|v=i} X_p^{\frac{1-Z_{vj}}{2} + \frac{1-Z_{vk}}{2} + \frac{1-Z_{vl}}{2}}, \end{aligned} \quad (\text{D4})$$

$$\mathbf{A}_v^{r1} = \prod_{p \supset v} X_p, \quad (\text{D5})$$

which matches Eqs. (B25)-(B26) of Ref. 1.

Next, we consider the \mathbf{B} terms. The \mathbf{B}_{∇}^Q is a projector that enforces $q_{ad}q_{du}\bar{q}_{au}$ around a triangle (adu) to be one. This is precisely the operator

$$\frac{1 + Z_{ad}Z_{du}Z_{au}}{2} = \frac{1 + \prod_{e \subset \nabla} Z_e}{2} \quad (\text{D6})$$

Lastly, we consider $\mathbf{B}_{c,x}^N$, which enforces

$$\omega(q_{ad}, q_{ds})\omega(q_{ad}, q_{dw})\omega(q_{ad}, q_{du}) \quad (\text{D7})$$

$$\omega(q_{ac}, q_{ct})\omega(q_{ac}, q_{cw})\omega(q_{ac}, q_{cu})n_y n_z n_{\bar{y}} n_{\bar{z}} = 1 \quad (\text{D8})$$

where we have removed the bars because $N = \mathbb{Z}_2$. Define

$$\begin{aligned} \mathbf{B}_{c,x}^r &= C Z_{ad,ds} C Z_{ad,dw} C Z_{ad,du} C Z_{ac,ct} C Z_{ac,cw} C Z_{ac,cu} \\ &Z_y Z_z Z_{\bar{y}} Z_{\bar{z}} \end{aligned} \quad (\text{D9})$$

where $CZ = \text{diag}(1, 1, 1, -1)$ is the controlled-Z operator. The operator above satisfies the above constraint exactly when its eigenvalue is one. Therefore, we see that the projector can be written as

$$\mathbf{B}_{c,x}^N = \frac{1 + \mathbf{B}_{c,x}^r}{2}. \quad (\text{D10})$$

In Ref. 1, we instead have the projector $\frac{1 + \mathbf{B}_{c,x} + \mathbf{B}_{c,x}^2 + \mathbf{B}_{c,x}^3}{4}$ where

$$\mathbf{B}_{c,x} = S_{ad} S_{at} S_{ds} S_{du} S_{cw} S_{ac}^\dagger S_{as}^\dagger S_{dw}^\dagger S_{cu}^\dagger S_{ct}^\dagger Z_y Z_z Z_{\bar{y}} Z_{\bar{z}} \quad (\text{D11})$$

These two projectors are not equal. Physically, this came from the fact that we started with different plaquette terms that commuted with the $(\mathbb{Z}_4, \mathbb{Z}_2)$ symmetry in the paramagnet. Nevertheless, we can verify via an explicit calculation that

$$\mathbf{B}_{c,x}^N \prod_{\nabla_{Cc}} \mathbf{B}_{\nabla}^Q = \frac{1 + \mathbf{B}_{c,x} + \mathbf{B}_{c,x}^2 + \mathbf{B}_{c,x}^3}{4} \prod_{\nabla_{Cc}} \mathbf{B}_{\nabla}^Q \quad (\text{D12})$$

That is, the projectors are equivalent in the $\mathbf{B}_{\nabla}^Q = 1$ subspace. Therefore, we conclude that although the Hamiltonians are different, the two models have exactly the same ground state.

2. (S_3, \mathbb{Z}_3)

Next, we present the simplest non-abelian hybrid fracton order, whose charges transform as irreps of S_3 (a similar construction is given in Ref. 36). We represent $N = \langle r | r^3 = 1 \rangle$ and $Q = \langle s | s^2 = 1 \rangle$. The group extension is a split extension whose factor system is given by $\sigma^s[r] = \bar{r}$ and trivial cocycle $\omega = 1$.

The operators on each edge can be represented by \mathbb{Z}_2 Pauli operators, while those on each plaquette are represented by \mathbb{Z}_3 clock and shift matrices \mathcal{Z} and \mathcal{X} , which satisfy $\mathcal{Z}\mathcal{X} = e^{2\pi i/3}\mathcal{X}\mathcal{Z}$. The automorphism operator acts as $\Sigma_p^s = \mathcal{C}_p$ where \mathcal{C} is the \mathbb{Z}_3 charge conjugation operator

$$\mathcal{C} = \begin{pmatrix} 1 & 0 & 0 \\ 0 & 0 & 1 \\ 0 & 1 & 0 \end{pmatrix} \quad (\text{D13})$$

Starting with \mathbf{A}_v^g , we can substitute

$$L_p^r = R_p^{\bar{r}} \equiv \mathcal{X}_p \quad (\text{D14})$$

$$R_p^r = L_p^{\bar{r}} \equiv \bar{\mathcal{X}}_p \quad (\text{D15})$$

$$R_e^s = L_e^s \equiv X_e \quad (\text{D16})$$

$$L_p^{\Sigma^e[r]} = R_p^{\Sigma^e[\bar{r}]} \equiv \mathcal{X}_p^{Z_e} \quad (\text{D17})$$

$$L_p^{\Sigma^e[\bar{r}]} = R_p^{\Sigma^e[r]} \equiv \bar{\mathcal{X}}_p^{Z_e} \quad (\text{D18})$$

With this, we find

$$\mathbf{A}_v^{1s} = \prod_{e \supset v} X_e \prod_{p|v=i} \mathcal{C}_p \quad (\text{D19})$$

$$\mathbf{A}_v^{\tau 1} = \prod_{p|v=j,l} \bar{\mathcal{X}}_p^{Z_{iv}} \prod_{p|v=k} \mathcal{X}_p^{Z_{iv}} \prod_{p|v=i} \mathcal{X}_p \quad (\text{D20})$$

The projector \mathbf{B}_{∇}^Q is the same as the previous case

$$\mathbf{B}_{\nabla}^Q = \frac{1 + \prod_{e \subset \nabla} Z_e}{2} \quad (\text{D21})$$

Lastly, the constraint of the cube operator $\mathbf{B}_{c,x}$ enforces

$$\sigma^{qac} [n_y] \sigma^{qad} [\bar{n}_z] \bar{n}_{\bar{y}} n_{\bar{z}} = 1 \quad (\text{D22})$$

Define the operator

$$\mathbf{B}_{c,x}^r = \mathcal{Z}_y^{Z_{ac}} \bar{\mathcal{Z}}_z^{Z_{ad}} \bar{\mathcal{Z}}_{\bar{y}} \mathcal{Z}_{\bar{z}} \quad (\text{D23})$$

which satisfies the constraint precisely when its eigenvalue is one. Therefore, the projector can be written as

$$\mathbf{B}_{c,x}^N = \frac{1 + \mathbf{B}_{c,x}^r + (\mathbf{B}_{c,x}^r)^2}{3} \quad (\text{D24})$$

3. (D_n, \mathbb{Z}_n)

The example of (D_n, \mathbb{Z}_n) is naturally obtained by generalizing the plaquette degrees of freedom in the (S_3, \mathbb{Z}_3) theory above to \mathbb{Z}_n qudits. Namely, the clock and shift matrices now satisfy $\mathcal{Z}\mathcal{X} = e^{2\pi i/n}\mathcal{X}\mathcal{Z}$, and the projector $\mathbf{B}_{c,x}^N$ is now given by

$$\mathbf{B}_{c,x}^N = \frac{1}{n} \sum_{m=1}^n (\mathbf{B}_{c,x}^r)^m \quad (\text{D25})$$

The model can be thought of as starting with the \mathbb{Z}_n X-cube model with degrees of freedom on the plaquettes, and gauging the charge conjugation symmetry, which results in a \mathbb{Z}_2 gauge field living on the edges.

4. (Q_8, \mathbb{Z}_4)

As a final example, we present the simplest non-abelian hybrid fracton model where the corresponding group extension is neither central nor split. The smallest group where this happens is $G = Q_8 = \langle r, s | r^4 = r^2 s^2 = (rs)^2 = 1 \rangle$ the quaternion group, $N = \mathbb{Z}_4 = \langle r | r^4 = 1 \rangle$, and $Q = \mathbb{Z}_2 = \langle s | s^2 = 1 \rangle$. The factor system is given by $\sigma^s[r] = \bar{r}$ and $\omega(s, s) = r^2$.

Each edge can be expressed using \mathbb{Z}_2 Pauli operators, while each plaquette can be expressed with \mathbb{Z}_4 clock and shift operators, which satisfy $\mathcal{Z}\mathcal{X} = i\mathcal{X}\mathcal{Z}$. The automorphism operator acts as $\Sigma_p^s = \mathcal{C}_p$, where \mathcal{C} is the \mathbb{Z}_4 charge conjugation operator

$$\mathcal{C} = \begin{pmatrix} 1 & 0 & 0 & 0 \\ 0 & 0 & 0 & 1 \\ 0 & 0 & 1 & 0 \\ 0 & 1 & 0 & 0 \end{pmatrix} \quad (\text{D26})$$

The substitution to Pauli operators for the A_v^g terms are

$$L_p^r = R_p^{\bar{r}} \equiv \mathcal{X}_p \quad (\text{D27})$$

$$R_p^r = L_p^{\bar{r}} \equiv \bar{\mathcal{X}}_p \quad (\text{D28})$$

$$R_e^s = L_e^{\bar{s}} \equiv X_e \quad (\text{D29})$$

$$L_p^{\Sigma^e[r]} = R_p^{\Sigma^e[\bar{r}]} \equiv \mathcal{X}_p^{Z_e} \quad (\text{D30})$$

$$L_p^{\Sigma^e[\bar{r}]} = R_p^{\Sigma^e[r]} \equiv \bar{\mathcal{X}}_p^{Z_e} \quad (\text{D31})$$

$$L_p^{\Omega(e,s)} = R_p^{\Omega(e,\bar{s})} \equiv (\mathcal{X}_p^2)^{\frac{1-Z_e}{2}} = \mathcal{X}_p^{1-Z_e} \quad (\text{D32})$$

Therefore, we have

$$A_v^{1s} = \prod_{p|v=j,k,l} \mathcal{X}_p^{1-Z_{iv}} \times \prod_{e \supset v} X_e \times \prod_{p|v=i} \mathcal{X}_p^{Z_{vj}-Z_{vk}+Z_{vl}-1} \mathcal{C}_p. \quad (\text{D33})$$

$$A_v^{r1} = \prod_{p|v=j,l} \bar{\mathcal{X}}_p^{Z_{iv}} \prod_{p|v=k} \mathcal{X}_p^{Z_{iv}} \prod_{p|v=i} \mathcal{X}_p \quad (\text{D34})$$

The projector B_{∇}^Q is again

$$B_{\nabla}^Q = \frac{1 + \prod_{e \subset \nabla} Z_e}{2} \quad (\text{D35})$$

Lastly, to express $B_{c,x}^N$ we define

$$B_{c,x}^r = CZ_{ad,ds} CZ_{ad,dw} CZ_{ad,du} CZ_{ac,ct} CZ_{ac,cw} CZ_{ac,cu} \\ Z_y^{Z_{ac}} \bar{Z}_z^{Z_{ad}} \bar{Z}_{\bar{y}} \bar{Z}_{\bar{z}} \quad (\text{D36})$$

which enforces the constraint when $B_{c,x}^r = 1$. Therefore, the projector is given by

$$B_{c,x}^N = \frac{1 + B_{c,x}^r + (B_{c,x}^r)^2 + (B_{c,x}^r)^3}{4} \quad (\text{D37})$$

The above construction can be straightforwardly generalized to any dicyclic group $(Q_{4n}, \mathbb{Z}_{2n})$ by replacing each plaquette with \mathbb{Z}_{2n} qudits.

-
- [1] N. Tantivasadakarn, W. Ji, and S. Vijay, Hybrid fracton phases: Parent orders for liquid and non-liquid quantum phases (2021), [arXiv:2102.09555 \[cond-mat.str-el\]](https://arxiv.org/abs/2102.09555).
- [2] C. Nayak, S. H. Simon, A. Stern, M. Freedman, and S. Das Sarma, Non-abelian anyons and topological quantum computation, *Rev. Mod. Phys.* **80**, 1083 (2008).
- [3] A. Y. Kitaev, Fault-tolerant quantum computation by anyons, *Annals of Physics* **303**, 2 (2003).
- [4] H. Bombin and M. A. Martin-Delgado, Statistical mechanical models and topological color codes, *Phys. Rev. A* **77**, 042322 (2008).
- [5] M. Levin and Z.-C. Gu, Braiding statistics approach to symmetry-protected topological phases, *Phys. Rev. B* **86**, 115109 (2012).
- [6] H. Moradi and X.-G. Wen, Universal topological data for gapped quantum liquids in three dimensions and fusion algebra for non-abelian string excitations, *Phys. Rev. B* **91**, 075114 (2015).
- [7] J. Haegeman, K. Van Acoleyen, N. Schuch, J. I. Cirac, and F. Verstraete, Gauging quantum states: From global to local symmetries in many-body systems, *Phys. Rev. X* **5**, 011024 (2015).
- [8] B. Yoshida, Gapped boundaries, group cohomology and fault-tolerant logical gates, *Annals of Physics* **377**, 387 (2017).
- [9] C. Chamon, Quantum glassiness in strongly correlated clean systems: An example of topological overprotection, *Phys. Rev. Lett.* **94**, 040402 (2005).
- [10] J. Haah, Local stabilizer codes in three dimensions without string logical operators, *Phys. Rev. A* **83**, 042330 (2011).
- [11] B. Yoshida, Exotic topological order in fractal spin liquids, *Phys. Rev. B* **88**, 125122 (2013).
- [12] S. Vijay, J. Haah, and L. Fu, A new kind of topological quantum order: A dimensional hierarchy of quasiparticles built from stationary excitations, *Phys. Rev. B* **92**, 235136 (2015).
- [13] S. Vijay, J. Haah, and L. Fu, Fracton topological order, generalized lattice gauge theory, and duality, *Phys. Rev. B* **94**, 235157 (2016).
- [14] E. Cobanera, G. Ortiz, and Z. Nussinov, The bond-algebraic approach to dualities, *Advances in physics* **60**, 679 (2011).
- [15] D. J. Williamson, Fractal symmetries: Ungauging the cubic code, *Phys. Rev. B* **94**, 155128 (2016).
- [16] A. Kubica and B. Yoshida, Ungauging quantum error-correcting codes, [arXiv preprint arXiv:1805.01836](https://arxiv.org/abs/1805.01836) (2018).
- [17] M. Pretko, The fracton gauge principle, *Phys. Rev. B* **98**, 115134 (2018).
- [18] W. Shirley, K. Slagle, and X. Chen, Foliated fracton order from gauging subsystem symmetries, *SciPost Phys.* **6**, 41 (2019).
- [19] D. Radicevic, Systematic constructions of fracton theories, [arXiv preprint arXiv:1910.06336](https://arxiv.org/abs/1910.06336) (2019).
- [20] S. Vijay and L. Fu, A generalization of non-abelian anyons in three dimensions (2017), [arXiv:1706.07070 \[cond-mat.str-el\]](https://arxiv.org/abs/1706.07070).
- [21] A. Prem, S.-J. Huang, H. Song, and M. Hermele, Cage-net fracton models, *Phys. Rev. X* **9**, 021010 (2019).
- [22] D. Aasen, D. Bulmash, A. Prem, K. Slagle, and D. J. Williamson, Topological defect networks for fractons of all types, *Phys. Rev. Research* **2**, 043165 (2020).
- [23] X.-G. Wen, Systematic construction of gapped nonliquid states, *Phys. Rev. Research* **2**, 033300 (2020).
- [24] J. Wang, Non-liquid cellular states, [arXiv preprint arXiv:2002.12932](https://arxiv.org/abs/2002.12932) (2020).
- [25] D. J. Williamson and M. Cheng, Designer non-abelian fractons from topological layers, [arXiv preprint arXiv:2004.07251](https://arxiv.org/abs/2004.07251) (2020).
- [26] H. Song, A. Prem, S.-J. Huang, and M. A. Martin-Delgado, Twisted fracton models in three dimensions, *Phys. Rev. B* **99**, 155118 (2019).
- [27] D. T. Stephen, J. Garre-Rubio, A. Dua, and D. J. Williamson, Subsystem symmetry enriched topological order in three dimensions, *Phys. Rev. Research* **2**, 033331 (2020).
- [28] D. Bulmash and M. Barkeshli, Gauging fractons: Immobile non-abelian quasiparticles, fractals, and position-dependent degeneracies, *Phys. Rev. B* **100**, 155146 (2019).
- [29] A. Prem and D. J. Williamson, Gauging permutation symmetries as a route to non-Abelian fractons, *SciPost Phys.* **7**, 68 (2019).
- [30] J. Wang and K. Xu, Higher-rank tensor field theory of non-abelian fracton and embeddon, *Annals of Physics* **424**, 168370 (2019).

- [31] J. Wang, K. Xu, and S.-T. Yau, Higher-rank tensor non-abelian field theory: Higher-moment or subdimensional polynomial global symmetry, algebraic variety, noether's theorem, and gauging, *Phys. Rev. Research* **3**, 013185 (2021).
- [32] J. Wang and S.-T. Yau, Non-abelian gauged fracton matter field theory: Sigma models, superfluids, and vortices, *Phys. Rev. Research* **2**, 043219 (2020).
- [33] W. Shirley, K. Slagle, Z. Wang, and X. Chen, Fracton models on general three-dimensional manifolds, *Phys. Rev. X* **8**, 031051 (2018).
- [34] W. Shirley, K. Slagle, and X. Chen, Universal entanglement signatures of foliated fracton phases, *SciPost Phys.* **6**, 15 (2019).
- [35] W. Shirley, K. Slagle, and X. Chen, Fractional excitations in foliated fracton phases, *Annals of Physics* **410**, 167922 (2019).
- [36] Y.-T. Tu and P.-Y. Chang, Non-abelian fracton order from gauging a semidirect product of subsystem and global symmetries, arXiv preprint arXiv:2103.08603 (2021).
- [37] J. Haah, Bifurcation in entanglement renormalization group flow of a gapped spin model, *Phys. Rev. B* **89**, 075119 (2014).
- [38] A. Dua, P. Sarkar, D. J. Williamson, and M. Cheng, Bifurcating entanglement-renormalization group flows of fracton stabilizer models, *Phys. Rev. Research* **2**, 033021 (2020).
- [39] P.-S. Hsin and K. Slagle, Comments on foliated gauge theories and dualities in $3+1$ d, arXiv preprint arXiv:2105.09363 (2021).
- [40] A. Kapustin and R. Thorngren, Higher symmetry and gapped phases of gauge theories, in *Algebra, Geometry, and Physics in the 21st Century* (Springer, 2017) pp. 177–202.
- [41] C. Delcamp and A. Tiwari, From gauge to higher gauge models of topological phases, *Journal of High Energy Physics* **2018**, 49 (2018).
- [42] C. Córdova, T. T. Dumitrescu, and K. Intriligator, Exploring 2-group global symmetries, *Journal of High Energy Physics* **2019**, 184 (2019).
- [43] F. Benini, C. Córdova, and P.-S. Hsin, On 2-group global symmetries and their anomalies, *Journal of High Energy Physics* **2019**, 1 (2019).
- [44] M. Barkeshli, P. Bonderson, M. Cheng, and Z. Wang, Symmetry fractionalization, defects, and gauging of topological phases, *Phys. Rev. B* **100**, 115147 (2019).
- [45] M. Hermele, String flux mechanism for fractionalization in topologically ordered phases, *Phys. Rev. B* **90**, 184418 (2014).
- [46] N. Tarantino, N. H. Lindner, and L. Fidkowski, Symmetry fractionalization and twist defects, *New Journal of Physics* **18**, 035006 (2016).
- [47] Y.-A. Chen, T. D. Ellison, and N. Tantivasadakarn, Disentangling supercohomology symmetry-protected topological phases in three spatial dimensions, *Phys. Rev. Research* **3**, 013056 (2021).
- [48] D. V. Else and C. Nayak, Classifying symmetry-protected topological phases through the anomalous action of the symmetry on the edge, *Phys. Rev. B* **90**, 235137 (2014).
- [49] S. Jiang, A. Mesaros, and Y. Ran, Generalized modular transformations in $(3+1)$ D topologically ordered phases and triple linking invariant of loop braiding, *Phys. Rev. X* **4**, 031048 (2014).
- [50] J. C. Wang and X.-G. Wen, Non-abelian string and particle braiding in topological order: Modular $SL(3, \mathbb{Z})$ representation and $(3+1)$ -dimensional twisted gauge theory, *Phys. Rev. B* **91**, 035134 (2015).
- [51] C. Delcamp, Excitation basis for $(3+1)$ d topological phases, *Journal of High Energy Physics* **2017**, 128 (2017).
- [52] T. Lan, L. Kong, and X.-G. Wen, Classification of $(3+1)$ D bosonic topological orders: The case when pointlike excitations are all bosons, *Phys. Rev. X* **8**, 021074 (2018).
- [53] C. Wang and M. Levin, Braiding statistics of loop excitations in three dimensions, *Phys. Rev. Lett.* **113**, 080403 (2014).
- [54] C.-M. Jian and X.-L. Qi, Layer construction of 3d topological states and string braiding statistics, *Phys. Rev. X* **4**, 041043 (2014).
- [55] C. Wang and M. Levin, Topological invariants for gauge theories and symmetry-protected topological phases, *Phys. Rev. B* **91**, 165119 (2015).
- [56] P. Putrov, J. Wang, and S.-T. Yau, Braiding statistics and link invariants of bosonic/fermionic topological quantum matter in $2+1$ and $3+1$ dimensions, *Annals of Physics* **384**, 254 (2017).
- [57] M. Cheng, N. Tantivasadakarn, and C. Wang, Loop braiding statistics and interacting fermionic symmetry-protected topological phases in three dimensions, *Phys. Rev. X* **8**, 011054 (2018).
- [58] Q.-R. Wang, M. Cheng, C. Wang, and Z.-C. Gu, Topological quantum field theory for abelian topological phases and loop braiding statistics in $(3+1)$ -dimensions, *Phys. Rev. B* **99**, 235137 (2019).
- [59] A. P. O. Chan, P. Ye, and S. Ryu, Braiding with borromean rings in $(3+1)$ -dimensional spacetime, *Phys. Rev. Lett.* **121**, 061601 (2018).
- [60] J.-R. Zhou, Q.-R. Wang, C. Wang, and Z.-C. Gu, Non-abelian three-loop braiding statistics for 3d fermionic topological phases, *Nature Communications* **12**, 3191 (2021).
- [61] Z.-F. Zhang and P. Ye, Compatible braidings with hopf links, multiloop, and borromean rings in $(3+1)$ -dimensional spacetime, *Phys. Rev. Research* **3**, 023132 (2021).
- [62] C. G. Brell, Generalized cluster states based on finite groups, *New Journal of Physics* **17**, 023029 (2015).
- [63] A. Mesaros and Y. Ran, Classification of symmetry enriched topological phases with exactly solvable models, *Phys. Rev. B* **87**, 155115 (2013).
- [64] D. Ben-Zion, D. Das, and J. McGreevy, Exactly solvable models of spin liquids with spinons, and of three-dimensional topological paramagnets, *Phys. Rev. B* **93**, 155147 (2016).
- [65] C. Heinrich, F. Burnell, L. Fidkowski, and M. Levin, Symmetry-enriched string nets: Exactly solvable models for set phases, *Phys. Rev. B* **94**, 235136 (2016).
- [66] M. Cheng, Z.-C. Gu, S. Jiang, and Y. Qi, Exactly solvable models for symmetry-enriched topological phases, *Phys. Rev. B* **96**, 115107 (2017).
- [67] D. J. Williamson, N. Bultinck, and F. Verstraete, Symmetry-enriched topological order in tensor networks: Defects, gauging and anyon condensation, arXiv preprint arXiv:1711.07982 (2017).
- [68] J. Garre-Rubio and S. Iblisdir, Local order parameters for symmetry fractionalization, *New Journal of Physics* **21**, 113016 (2019).